

University of Nebraska - Lincoln

DigitalCommons@University of Nebraska - Lincoln

Biological Systems Engineering: Papers and Publications

Biological Systems Engineering

2010

Net Radiation Dynamics: Performance of 20 Daily Net Radiation Models as Related to Model Structure and Intricacy in Two Climates

Suat Irmak

University of Nebraska-Lincoln, suat.irmak@unl.edu

Denis Mutiibwa

University of Nebraska-Lincoln, mutiibwa2000@yahoo.com

José O. Payero

University of Nebraska-Lincoln, jpayero@clemsun.edu

Follow this and additional works at: <https://digitalcommons.unl.edu/biosysengfacpub>

 Part of the [Biological Engineering Commons](#)

Irmak, Suat; Mutiibwa, Denis; and Payero, José O., "Net Radiation Dynamics: Performance of 20 Daily Net Radiation Models as Related to Model Structure and Intricacy in Two Climates" (2010). *Biological Systems Engineering: Papers and Publications*. 235.
<https://digitalcommons.unl.edu/biosysengfacpub/235>

This Article is brought to you for free and open access by the Biological Systems Engineering at DigitalCommons@University of Nebraska - Lincoln. It has been accepted for inclusion in Biological Systems Engineering: Papers and Publications by an authorized administrator of DigitalCommons@University of Nebraska - Lincoln.

NET RADIATION DYNAMICS: PERFORMANCE OF 20 DAILY NET RADIATION MODELS AS RELATED TO MODEL STRUCTURE AND INTRICACY IN TWO CLIMATES

S. Irmak, D. Mutiibwa, J. O. Payero

ABSTRACT. We compared daily net radiation (R_n) estimates from 19 methods with the ASCE-EWRI R_n estimates in two climates: Clay Center, Nebraska (sub-humid) and Davis, California (semi-arid) for the calendar year. The performances of all 20 methods, including the ASCE-EWRI R_n method, were then evaluated against R_n data measured over a non-stressed maize canopy during two growing seasons in 2005 and 2006 at Clay Center. Methods differ in terms of inputs, structure, and equation intricacy. Most methods differ in estimating the cloudiness factor, emissivity (ϵ), and calculating net longwave radiation (R_{nl}). All methods use albedo (α) of 0.23 for a reference grass/alfalfa surface. When comparing the performance of all 20 R_n methods with measured R_n , we hypothesized that the α values for grass/alfalfa and non-stressed maize canopy were similar enough to only cause minor differences in R_n and grass- and alfalfa-reference evapotranspiration (ET_o and ET_r) estimates. The measured seasonal average α for the maize canopy was 0.19 in both years. Using $\alpha = 0.19$ instead of $\alpha = 0.23$ resulted in 6% overestimation of R_n . Using $\alpha = 0.19$ instead of $\alpha = 0.23$ for ET_o and ET_r estimations, the 6% difference in R_n translated to only 4% and 3% differences in ET_o and ET_r , respectively, supporting the validity of our hypothesis. Most methods had good correlations with the ASCE-EWRI R_n ($r^2 > 0.95$). The root mean square difference (RMSD) was less than $2 \text{ MJ m}^{-2} \text{ d}^{-1}$ between 12 methods and the ASCE-EWRI R_n at Clay Center and between 14 methods and the ASCE-EWRI R_n at Davis. The performance of some methods showed variations between the two climates. In general, r^2 values were higher for the semi-arid climate than for the sub-humid climate. Methods that use dynamic ϵ as a function of mean air temperature performed better in both climates than those that calculate ϵ using actual vapor pressure. The ASCE-EWRI-estimated R_n values had one of the best agreements with the measured R_n ($r^2 = 0.93$, $\text{RMSD} = 1.44 \text{ MJ m}^{-2} \text{ d}^{-1}$), and estimates were within 7% of the measured R_n . The R_n estimates from six methods, including the ASCE-EWRI, were not significantly different from measured R_n . Most methods underestimated measured R_n by 6% to 23%. Some of the differences between measured and estimated R_n were attributed to the poor estimation of R_{nl} . We conducted sensitivity analyses to evaluate the effect of R_{nl} on R_n , ET_o , and ET_r . The R_{nl} effect on R_n was linear and strong, but its effect on ET_o and ET_r was subsidiary. Results suggest that the R_n data measured over green vegetation (e.g., irrigated maize canopy) can be an alternative R_n data source for ET estimations when measured R_n data over the reference surface are not available. In the absence of measured R_n , another alternative would be using one of the R_n models that we analyzed when all the input variables are not available to solve the ASCE-EWRI R_n equation. Our results can be used to provide practical information on which method to select based on data availability for reliable estimates of daily R_n in climates similar to Clay Center and Davis.

Keywords. Albedo, Alfalfa-reference evapotranspiration, Evapotranspiration, Grass-reference evapotranspiration, Maize, Net radiation, Penman-Monteith.

Net radiation (R_n) is the difference between total downwelling and upwelling radiation fluxes and is a measure of the radiant energy exchange at the earth's surface. It is one of the primary driving

forces in the surface energy balance, including latent heat (evapotranspiration, ET), and other biological and biophysical processes. Most ET equations and micrometeorological and surface-atmosphere energy exchange studies require R_n . The accuracy of the estimations of ET and other dynamics of energy exchange mechanisms depends on accurate quantification of this variable. Limitations in measured R_n data have been a persistent problem in studies involving land surface-atmosphere interactions, hydrologic modeling, micrometeorology, and water resources management in agro-ecological landscapes. Although the number of automated weather stations that monitor major climate variables has been increasing in the last two decades, the number of weather stations that have net radiometers is still limited because direct measurement of R_n is an expensive task and involves vigorous maintenance for the net radiometers. Thus, estimation of R_n from air temperature, total incoming shortwave solar radiation (R_s), and other climatic variables remains the dominant approach in most parts of the U.S. and around the world. In the U.S., the ratio between stations measuring R_n

Submitted for review in August 2009 as manuscript number SW 8136; approved for publication by the Soil & Water Division of ASABE in June 2010.

The mention of trade names or commercial products is solely for the information of the reader and does not constitute an endorsement or recommendation for use by the University of Nebraska-Lincoln or the authors.

The authors are **Suat Irmak, ASABE Member Engineer**, Associate Professor, and **Denis Mutiibwa, ASABE Member Engineer**, Graduate Research Assistant, Department of Biological Systems Engineering, University of Nebraska-Lincoln, Lincoln, Nebraska; **José O. Payero**, Research Scientist, Irrigated Farming Systems, Department of Primary Industries and Fisheries, Toowoomba, Australia. **Corresponding author:** Suat Irmak, Department of Biological Systems Engineering, University of Nebraska-Lincoln, 241 L.W. Chase Hall, Lincoln, NE 68583; phone: 402-472-4865; fax: 402-472-6338; e-mail: sirmak2@unl.edu.

and those observing only primary climatic variables such as R_s , air temperature, relative humidity, and rainfall is approximately 1:100 (Thornton and Running, 1999). For example, the High Plains Regional Climate Center (Hubbard, 1992) operates approximately 70 weather stations throughout Nebraska and another approximately 120 automated weather stations in neighboring states, none of which monitor R_n . Furthermore, the density of weather stations that observe air temperature and R_s to estimate R_n is not nearly enough to make spatial estimates of R_n for determining spatial distribution of surface energy balance components in agro-ecological settings.

Adding to the issues involved with an insufficient density of stations that observe R_n , net radiometers are one of the most delicate sensors used in agro-meteorological stations. Extensive maintenance, cost, calibration, and other challenges, such as the variability between different brands of sensors and inaccuracies of the measurements when the sensor is moistened by rain, irrigation water, or dew formation, led to the development of methods to estimate R_n from surface characteristics and climatic variables. An additional difficulty is the requirement that R_n be measured over irrigated and well-maintained reference surfaces when used in grass- or alfalfa-reference ET (ET_o and ET_r , respectively) calculations. This is particularly difficult in arid and semi-arid regions, where maintaining a large number of irrigated and well-maintained reference surface sites of large enough size (i.e., ≥ 4 ha) for automated weather station networks is a formidable and very expensive task. One alternative approach would be to use R_n measured over other vegetation surfaces for ET estimations or to use microclimatic variables measured over other green vegetation surfaces to estimate R_n . In recent years, in addition to the automated weather stations, surface energy flux measurement systems, such as the Bowen ratio energy balance system (BREBS; Bowen, 1926; Tanner, 1960; Denmead and McIlroy, 1970; Fuchs and Tanner, 1970); eddy covariance system (ECS; Swinbank, 1951; Deacon and Swinbank, 1958; Tanner, 1960; Dyer, 1961; Webb et al., 1980; Aubinet et al., 2001; Finnigan et al., 2003); and surface renewal (SR; Paw et al., 1995; Snyder et al., 1996, 2008) are being used over various vegetation surfaces to monitor surface energy balance components, including R_n , for research and other purposes. Thus, the R_n and microclimatic measurements from these systems could be another potential source of data for R_n for ET estimations of other surfaces. In addition, in many cases, these surface energy balance systems are the only source of data to quantify R_n and/or ET for other surfaces due to absence of automated reference weather stations in the area for which the R_n and ET estimations are needed.

Numerous methods have been developed to estimate R_n . The models differ in the intricacy of their calibration structure and in their use of climatic parameters, variables, and coefficients. The primary differences among them revolve around the procedures used to compute clear-sky solar radiation, net outgoing longwave radiation, atmospheric emissivity, and actual vapor pressure of the air. A developed and tested robust set of equations has been compiled and published by the ASCE Environmental and Water Resources Institute (ASCE-EWRI, 2005), and these procedures have been suggested as the standardized procedures to estimate R_n (this method is referred to the ASCE-EWRI R_n method in our study). The ASCE-EWRI R_n calculation procedures have also been recommended for estimating ET_o and ET_r using

standardized ASCE-Penman-Monteith equation (ASCE-EWRI PM) (ASCE-EWRI, 2005).

Although the ASCE-EWRI approach for predicting R_n is widely used in the U.S. and around the world, studies that compare these procedures with other empirical procedures and with measured R_n data are limited. Most R_n methods, including the ASCE-EWRI, require measured R_s data. Use of measured R_s to compute R_n reduces the computational intensity and minimizes the error from calculating R_s using an estimation of relative sunshine duration (n/N , the ratio of actual measured bright sunshine hours and maximum possible sunshine hours). Relative sunshine duration is the ratio that indicates the cloudiness of the atmosphere, which was first proposed by Angström (1924) to estimate R_s . The net outgoing shortwave radiation (R_{so}) required for computing net longwave radiation (R_{nl}) can be estimated using a number of methods. The ASCE-EWRI (2005) recommends four methods to compute R_{so} depending on the calibration constants, air turbidity, and elevation. However, the ASCE-EWRI does not present an assessment of how different R_{nl} computations might impact R_n , ET_r , and ET_o . In addition, the ASCE-EWRI R_n procedure requires the input parameters of R_s , maximum and minimum air temperature (T_{max} and T_{min}), dew point temperature (T_{dew}), and maximum and minimum relative humidity (RH_{max} and RH_{min}). Given the limitations in availability and quality of climatic data, especially in developing countries, there is a need to evaluate the performance of different R_n calculation procedures relative to the ASCE-EWRI R_n method and measured R_n data. Although the ASCE-EWRI approach represents a standardized way of computing R_n , in many cases the availability and quality of input parameters dictate which R_n method can be used.

We compared daily R_n estimates from 19 methods to ASCE-EWRI R_n estimates in two climates: a transition zone between semi-humid and semi-arid climates at Clay Center, Nebraska, and a Mediterranean-type semi-arid climate at Davis, California. The performance of all 20 R_n methods, including the ASCE-EWRI R_n method, were then evaluated using measured R_n over a non-stressed maize canopy for Clay Center for two growing seasons in 2005 and 2006. In comparing the measured R_n over the maize canopy with the R_n estimated based on a grass-reference surface, our hypothesis was that the albedo (α) values of maize and grass and alfalfa ($\alpha = 0.23$) were similar and that minor differences in α (e.g., up to 20%) would not impact the R_n and ET estimations significantly. We tested this hypothesis by quantifying the impact of using different α values on R_n , ET_o , and ET_r . We also discuss the model performance in relation to the model structure and complexity.

MATERIALS AND METHODS

CLIMATE DATA AND STATISTICAL ANALYSES

The climate data measured at two locations were used: Clay Center, Nebraska (40° 34' N, 98° 8' W, 552 m above mean sea level, MSL) and Davis, California (38° 32' 09" N, 121° 46' 32" W, 18 m above MSL). Measured daily weather data for a 20-year period (1 January 1983 to 31 December 2004) at Clay Center and for a 14-year period (1 January 1990 to 31 December 2004) at Davis were used. Clay Center datasets were obtained from the High Plains Regional Climate Center (HPRCC; www.hprcc.unl.edu). Davis datasets were

obtained from the California Department of Water Resources, California Irrigation Management Information System (CIMIS) (Snyder and Pruitt, 1992) (www.cimis.water.ca.gov). The type of instrumentation and placement heights for each site were reported by Irmak et al. (2006). Weather variables measured at these stations included wind speed at 2 m height (u_2), T_{max} , T_{min} , RH_{max} , RH_{min} , rainfall, and R_s . The ASCE-EWRI R_n calculation procedures were used as the reference method to predict daily R_n . The R_n comparisons between ASCE-EWRI R_n vs. all other 19 methods were made on a daily basis for the two locations for the calendar year. The performances of all 20 R_n methods, including the ASCE-EWRI R_n method, were then compared with the measured data for Clay Center from 1 June to 30 September in 2005 and from 1 June to 20 September in 2006. The coefficient of determination (r^2), slope, and root mean square difference (RMSD) were computed to quantify over- and underpredictions and performance of each R_n method. A two-tailed t-test (for two-sample for means) was performed to identify whether R_n estimates from the 20 methods were significantly different from the measured R_n values at Clay Center at the 5% significance level. The null hypothesis was that the method-estimated and measured R_n values came from the same population and that the hypothesized (null hypothesis) mean difference between estimated and measured R_n values was zero. Further analyses were done to quantify the differences between method-estimated R_{nl} and ASCE-EWRI-estimated R_{nl} . We quantified the differences between the method-estimated R_{nl} , including the ASCE-EWRI R_{nl} , with the measured R_{nl} for Clay Center. Sensitivity analyses were conducted to quantify the sensitivity of R_n , ET_o , and ET_r to R_{nl} , and also to evaluate the sensitivity of R_n , ET_o , and ET_r to α . Since the estimated R_n data from the 20 methods tested and the ASCE-EWRI estimated R_n data are time series data on a daily time step, there is a probability that autocorrelation (AC) exists between the method-estimated and ASCE-EWRI-estimated R_n data. More importantly, autocorrelation in the residuals of regression obtained from regression analysis of method-estimated R_n versus ASCE-EWRI R_n or in the paired differences of R_n estimates and measured R_n values may affect the estimation of regression parameter estimates (slope and intercept) and model RMSD, and/or the significance of paired t-tests, respectively. In order to investigate and address potential autocorrelation, regression models were constructed using PROC AUTOREG (SAS/STAT v. 9.2, SAS Institute, Inc., Cary, N.C.), and the residuals of the R_n data were tested for each method. The Durbin-Watson test was used to check for the first-order autocorrelation of the residuals.

GENERAL FIELD EXPERIMENTAL PROCEDURES

Field experiments for measurements of R_n were conducted at the University of Nebraska-Lincoln, South Central Agricultural Laboratory (SCAL) near Clay Center, Nebraska, in 2005 and 2006. SCAL is located approximately 160 km west of Lincoln in the south central part of the state. The R_n measurements were made over a non-stressed maize (*Zea mays* L.) canopy. We hypothesized that the maize had a similar α value as the grass- or alfalfa-reference surface and that using R_n measured above the maize canopy would not significantly influence the ET estimations when R_n was estimated with the 19 methods as compared with the measured values.

Maize (hybrid Pioneer 33B51 with a comparative relative maturity of 113 days) was planted at 0.76 m row spacing with a seeding rate of approximately 73,000 seeds ha^{-1} and a planting depth of 0.05 m in an east-west row direction. In 2005, maize was planted on 22 April, emerged on 12 May, matured on 7 September, and was harvested on 17 October. In 2006, maize was planted on 12 May, emerged on 20 May, matured on 13 September, and was harvested on 5 October. The hybrid had 2,730 growing degree units to black layer with 113 to 114 days to maturity and was a non-prolific hybrid that had flex ear characteristics (ear length changes in response to environmental characteristics). The maximum maize height was measured as 2.50 m on 20 July 2005 and 31 July 2006. The experimental field (13.8 ha) was irrigated with subsurface drip irrigation system. Detailed descriptions of the additional experimental site and soil and plant management practices were reported by Irmak et al. (2008) and Irmak and Mutibwa (2008). Drip laterals were spaced every 1.5 m (every other plant row) in the middle of the furrow and were installed approximately 0.40 m below the soil surface. Irrigations were applied three times a week to meet the plant water requirement. A total of 225 and 172 mm of irrigation water was applied during the 2005 and 2006 growing seasons, respectively. A total of 283 and 330 mm of rainfall occurred during the growing season in 2005 and 2006, respectively.

FIELD MEASUREMENT OF RADIATION ENVELOPES

Net radiation and other microclimatic variables in the maize field were measured using a deluxe version of a Bowen ratio energy balance system (BREBS; Radiation and Energy Balance Systems, REBS, Inc., Bellevue, Wash.). The BREBS and data used in this study are part of the Nebraska Water and Energy Flux Measurement, Modeling and Research Network (NEBFLUX) (Irmak, 2010) that operates ten deluxe version of BREBS and one eddy covariance system over various vegetation surfaces ranging from irrigated and rainfed grasslands, tilled and untilled, and irrigated and rainfed croplands to Phragmites (*Phragmites australis*)-dominated cottonwood (*Populus deltoides* var. *occidentalis*) and willow stand (*Willow salix*) plant communities. Detailed description of the microclimate measurements, including latent heat flux, sensible heat flux, soil heat flux, net radiation, and other microclimatic variables (vapor pressure, air temperature, relative humidity, wind speed and direction, incoming and outgoing shortwave radiation, albedo, and soil temperature) were presented by Irmak (2010) and only a brief description of some of the primary measurements using the BREBS will be presented here. R_n was measured using a REBS Q*7.1 net radiometer that was installed approximately 4.5 m above the canopy. The radiometer is sensitive to wavelengths from 0.25 to 60 μm . It is attached to a 4 m long metal arm to extend the radiometer away from the tripod (horizontally to the plant canopy) so that only the R_n at the canopy/soil surface is measured and the reflection of heat and radiation from any other instruments and equipment (i.e., solar panel, etc.) installed on the tripod is eliminated. The net radiometer had two type-E chromel-constantan differential thermocouple junctions that are installed to monitor temperature differences between the core and upper and lower windshields (domes). The net radiometer was supplied with constant air blown through a desiccant tube to keep the air inside the dome dry so that formation of condensation inside the dome was eliminated. Incoming and outgoing shortwave and long-

wave radiation were measured simultaneously using a REBS model THRDS7.1 double-sided total hemispherical radiometer that was sensitive to wavelengths from 0.25 to 60 μm . The surface α was calculated as the ratio of outgoing shortwave to incoming shortwave radiation. All variables were sampled at 30 s intervals and then averaged and recorded every hour using a model CR10X datalogger and AM416 relay multiplexer (Campbell Scientific, Logan, Utah). The BREBS maintenance on a weekly basis included cleaning the thermocouples, servicing the radiometers by cleaning or replacing the domes, checking/replacing the desiccant tubes, and making sure that the net and solar radiometers were properly leveled.

ASCE-EWRI R_n CALCULATION PROCEDURES

The ASCE-EWRI R_n calculation procedures as outlined in ASCE-EWRI (2005) are as follows:

$$R_n = R_{ns} \downarrow - R_{nl} \uparrow \quad (1)$$

where

- R_n = net radiation ($\text{MJ m}^{-2} \text{d}^{-1}$)
- R_{ns} = incoming net shortwave radiation ($\text{MJ m}^{-2} \text{d}^{-1}$)
- R_{nl} = outgoing net longwave radiation ($\text{MJ m}^{-2} \text{d}^{-1}$).

The R_{ns} is a result of the balance between incoming and reflected solar radiation as a function of α :

$$R_{ns} = (1 - \alpha)R_s \downarrow \quad (2)$$

where

- α = albedo or canopy reflection coefficient (fixed at 0.23 for a green vegetation surface)
- R_s = total incoming shortwave solar radiation ($\text{MJ m}^{-2} \text{d}^{-1}$).

The rate of R_{nl} is proportional to the fourth power of the absolute temperature of the surface:

$$R_{nl} = \sigma \left[\frac{T_{max,K}^4 + T_{min,K}^4}{2} \right] (0.34 - 0.14\sqrt{e_a}) \times \left(1.35 \frac{R_s}{R_{so}} - 0.35 \right) \quad (3)$$

where

- σ = Stefan-Boltzmann constant ($4.903 \times 10^{-9} \text{ MJ K}^{-4} \text{ m}^{-2} \text{ d}^{-1}$)
- $T_{max,K}$ = daily maximum absolute air temperature ($\text{K} = ^\circ\text{C} + 273.16$)
- $T_{min,K}$ = daily minimum absolute air temperature ($\text{K} = ^\circ\text{C} + 273.16$)
- e_a = actual vapor pressure of the air (kPa)
- R_{so} = calculated clear-sky solar radiation ($\text{MJ m}^{-2} \text{d}^{-1}$).

The actual vapor pressure is calculated as:

$$e_a = 0.6108 \exp \left[\frac{17.27T_{dew}}{T_{dew} + 237.3} \right] \quad (4)$$

where T_{dew} is the dew point temperature ($^\circ\text{C}$). Depending on the availability of data, e_a can be calculated using RH and/or T_{min} .

Doorenbos and Pruitt (1977) developed an equation to calculate daily values of R_{so} as a function of station elevation (z , m) and extraterrestrial radiation (Ra , $\text{MJ m}^{-2} \text{d}^{-1}$) as:

$$R_{so} = (0.75 + 2 \times 10^{-5} z) Ra \downarrow \quad (5)$$

Daily Ra ($\text{MJ m}^{-2} \text{d}^{-1}$) can be calculated as a function of day of the year, solar constant and declination, and latitude:

$$Ra = \frac{1440}{\pi} G_{sc} d_r \times [\omega_s \sin(\varphi) \sin(\delta) + \cos(\varphi) \cos(\delta) \sin(\omega_s)] \quad (6)$$

where

- G_{sc} = solar constant ($0.0820 \text{ MJ m}^{-2} \text{min}^{-1}$)
- d_r = inverse relative distance from earth to sun
- ω_s = sunset hour angle (rad)
- φ = latitude (rad)
- δ = solar declination (rad)

$$\delta = 0.4093 \sin \left(\frac{2\pi(284 + J)}{365} \right) \quad (7)$$

where J is the day of the year (1 to 366)

$$d_r = 1 + 0.033 \cos \left(\frac{2\pi J}{365} \right) \quad (8)$$

$$\omega_s = \arccos(\psi) \quad (9)$$

$$\psi = \tan(\varphi) \tan(\delta) \quad (10)$$

NET RADIATION CALCULATION PROCEDURE FOR 19 OTHER R_n METHODS

The following section provides brief background information and describes the general procedures and common equations used in the different R_n methods for the calculation of various parameters and variables. Descriptions of the equation structure, coefficients, and variables used for each R_n method are provided later in this article. Dew point temperature, used in equation 4 to compute e_a , was not measured at either study location and was computed using the following equation (Murray, 1967):

$$T_{dew(i)} = \frac{237.3}{\left[1 / \left(\frac{\ln RH_i}{17.27} \right) + \left(\frac{T_i}{237.3} + T_i \right) \right]^{-1}} \quad (11)$$

where RH_i is the mean relative humidity (%) for period i , and T_i is the mean temperature ($(T_{max} + T_{min})/2$, $^\circ\text{C}$) for period i .

Net shortwave radiation (R_{ns}) is the balance of incoming and reflected solar radiation. R_s can be calculated using Angström's formula, as recommended by Doorenbos and Pruitt (1977):

$$R_s = \left(0.25 + 0.5 \frac{n}{N} \right) Ra \quad (12)$$

where n/N is the ratio of actual measured bright sunshine hours and maximum possible sunshine hours. Besides the

temperature and humidity, R_{nl} is influenced by cloudiness and by the difference between temperatures of the surface and the air. Jensen et al. (1990) presented a general formula for calculating R_{nl} :

$$R_{nl} = f\varepsilon\sigma T^4 \quad (13)$$

where σ is the Stefan-Boltzmann constant (4.895×10^{-9} MJ $m^{-2} d^{-1} K^{-4}$), T is the average air temperature, f is a factor to adjust for cloud cover, and ε is the atmospheric emissivity. Wright and Jensen et al. (1972) proposed the following equation for f :

$$f = a \frac{R_s}{R_{so}} + b \quad (14)$$

and Brunt (1932) developed an empirical equation for atmospheric ε :

$$\varepsilon = a_1 + b_1 \sqrt{e_a} \quad (15)$$

where $a = 1.35$, $b = -0.34$, $a_1 = 0.35$, and $b_1 = -0.14$; e_a is calculated using equation 4.

Wright (1982) presented an approach for dynamic values of a , b , and a_1 :

for $R_s/R_{so} > 0.7$: $a = 1.126$ and $b = -0.07$

for $R_s/R_{so} \leq 0.7$: $a = 1.017$ and $b = -0.06$.

$$a_1 = 0.26 + 0.1 \exp\left\{-\left(0.0154(30m + N - 207)\right)^2\right\} \quad (16)$$

where m is the month, and N is the day of year

Another equation, which requires only mean air temperature to estimate ε , was presented by Idso et al. (1969) and Idso and Jackson (1969):

$$\varepsilon = -0.02 + 0.261 \exp[-7.77 \times 10^{-4} (273 - T)^2] \quad (17)$$

To compute f to adjust for cloud cover, one can obtain estimated values of R_{so} by plotting observed R_s values to obtain an envelope curve through the maximum radiation values. Allen et al. (1998) presented two procedures to calculate R_{so} . If the calibrated values of a_s and b_s are available, equation 18 is recommended:

$$R_{so} = (a_s + b_s) R_a \quad (18)$$

Doorenbos and Pruitt (1977) recommended using 0.25 and 0.50 for a_s and b_s , respectively. For areas with high turbidity or when the sun angle is less than 50° , Allen et al. (1998) recommended equation 19 to calculate R_{so} . This equation is applicable when the calibrated values are not available only for station elevations less than 6,000 m having low air turbidity:

$$R_{so} = R_a \exp\left(\frac{-0.0018P}{K_t \sin \phi}\right) \quad (19)$$

where P is the atmospheric pressure (kPa), K_t is the turbidity coefficient ($0 < K_t \leq 1.0$; 1.0 for clean air; and 0.1 for extremely turbid, dusty, or polluted air), and ϕ is the sun angle above the horizon (rad). For daily calculations, ϕ can be determined as:

$$\sin \phi_{24} =$$

$$\sin \left[0.85 + 0.3\phi \sin \left(\frac{2\pi}{365} J - 1.39 \right) - 0.42\phi^2 \right] \quad (20)$$

where ϕ_{24} is average sun angle during the daylight period, weighted according to R_a .

Allen (1997) suggested that the estimation for R_{so} can be improved by considering the effect of water vapor on shortwave absorption, as incorporated into equation 21:

$$R_{so} = (K_B + K_D) R_a \quad (21)$$

where K_B is the clearness index for direct beam radiation, and K_D is the corresponding index for diffuse beam radiation and is computed as:

$$K_B = 0.98 \exp \left[\frac{-0.00146P}{K_t \sin \phi} - 0.091 \left(\frac{W}{\sin \phi} \right)^{0.25} \right] \quad (22)$$

$$W = 0.14e_a P + 2.1 \quad (23)$$

where W is the precipitable water vapor in the atmosphere (mm), and all other parameters have been previously defined. K_D is estimated from K_B as:

$$K_D = 0.35 - 0.33K_B \text{ for } K_B \geq 0.15 \quad (24)$$

$$K_D = 0.18 + 0.82K_B \text{ for } K_B < 0.15 \quad (25)$$

Using a cosine function and data from NOAA (1977-1980) for the western U.S., Heermann et al. (1985) derived an empirical equation to describe daily R_{so} (MJ $m^{-2} d^{-1}$) for the calendar year:

$$R_{so} = A' + B' \cos \left[\frac{2\pi J}{365 - C'} \right] \quad (26)$$

where $A' = 31.55 - 0.273L + 0.0008A$ and $B' = -0.299 + 0.268L + 0.0004A$, where $L = \text{latitude } (^\circ)$ and $A = \text{altitude (m)}$. C' is a phase constant theoretically set to 2.92 and corresponds to the longest day of the year (21 June), and the cosine function is for values in radians. Jensen et al. (1990) developed a linear equation correlating R_n with R_s :

$$R_n = a_3 R_s + b_3 \quad (27)$$

where the regression coefficients, $a_3 = 0.61$ and $b_3 = -1.0$, were obtained by averaging data from 14 locations worldwide. With the objective of developing alternative equations to reduce the input and computational intensity for FAO Irrigation and Drainage Paper No. 56 (Allen et al., 1998) R_n calculation procedures, Irmak et al. (2003) derived two equations to predict daily R_n using minimum climatological data. The first equation (the measured R_s -based equation) requires T_{max} , T_{min} , measured R_s , and d_r as input parameters:

$$R_n = (-0.054T_{max}) + (0.111T_{min}) + (0.462R_{s(measured)}) + (-49.243d_r) + 50.831 \quad (28)$$

where the units of T_{max} , T_{min} , and R_s (measured) are $^\circ C$, $^\circ C$, and MJ $m^{-2} d^{-1}$, respectively. The second equation (the predicted R_s -based equation) requires T_{max} , T_{min} , RH_{mean} , and predicted R_s :

$$R_n = (-0.09T_{\max}) + (0.203T_{\min}) - (0.101RH_{\min}) + (0.687R_{s(\text{predicted})}) + 3.97 \quad (29)$$

In equation 29, R_s is predicted using the Hargreaves and Samani (1982) and Samani (2000) equation:

$$R_s = (KT)(R_a)(TD)^{0.5} \quad (30)$$

where $TD = T_{\max} - T_{\min}$ ($^{\circ}\text{C}$), and KT is an empirical coefficient. Allen (1997) suggested using $KT = 0.17(P/P_o)^{0.5}$ for interior regions and $KT = 0.2(P/P_o)^{0.5}$ for coastal regions (elevations <1500 m), where P is mean monthly atmospheric pressure (kPa), and P_o is mean monthly atmospheric pressure at sea level (kPa).

Using equation 2, R_{ns} was estimated from measured R_s for Clay Center and Davis. To account for the effect of cloud cover and ϵ of the maize canopy, R_{nl} was estimated using equation 13 through 15. R_{nl} was also measured at Clay Center using the BREBS. Five different equations (eqs. 5, 18, 19, 21, and 26) were used to estimate R_{so} . R_{so} was also measured using the BREBS at Clay Center. Parameters a and b in equation 14, to adjust for cloud cover, were used both as constants and variables in the different R_n methods. The value of ϵ was computed using two equations (eqs. 15 and 17). Parameters a_1 and b_1 in equation 15 were also used as constants and variables by some of the R_n methods. The following section outlines the variables and constants used by each of the 19 methods to compute R_n . The structure of each R_n method, its input requirements, and its calculation steps are presented in table 1. All methods, except methods 15, 16, and 17, use the same form of equation 1 and calculate R_n as a difference between R_{ns} and R_{nl} . All methods, except methods 15, 16, and 17, use equation 2 to compute R_{ns} . Methods 15, 16, and 17 estimate R_n directly from R_s (i.e., R_{ns} is not calculated). Three of the 19 R_n methods use estimated

R_s . Methods 17, 18, and 19 use either equation 12 or equation 30 to estimate R_s using the n/N ratio and Ra as constants.

The following example illustrates how the 19 R_n methods were used to compute R_n as a function of different parameters and constants. As shown in table 1, method 1 uses measured R_s . The R_{so} for method 1 was calculated using equation 18. The R_{ns} was calculated as a function of α and R_s using equation 2. The R_{nl} was calculated using equation 13. Parameters a and b in the calculation of factor f were taken as constants ($a = 1.35$; $b = -0.34$). The net atmospheric emissivity (ϵ) was calculated using equation 17 as a function of air temperature. Equation 17 does not use parameters a_1 and b_1 . Finally, the daily R_n value for method 1 was calculated using the difference between R_{ns} and R_{nl} (eq. 1). Similar examples can be followed to identify which methods use which equations, constants, variables, or parameters to compute R_n . In table 1, the ASCE-EWRI R_n method is not listed because this method uses equations 1 through 10.

CALCULATION OF GRASS- AND ALFALFA- REFERENCE EVAPOTRANSPIRATION

The impact of different α values on ET_o and ET_r was determined by solving the ASCE-EWRI PM equation with two α values. The ASCE-EWRI PM equation is intended to simplify and clarify the application of the method and associated equations for computing aerodynamic and bulk surface resistance (r_a and r_s , respectively). Equations were combined into a single expression for grass- and alfalfa-reference surfaces and for a daily time step by varying coefficients. The equation as presented by ASCE-EWRI (2005) is:

$$ET_{ref} = \frac{0.408\Delta(R_n - G) + \gamma \frac{C_n}{T + 273} u_2 (e_s - e_a)}{[\Delta + \gamma(1 + C_d u_2)]} \quad (31)$$

Table 1. Structure of the methods used to compute R_n as a function of variables, constants, and equations.^[a]

R_n Method	R_{ns} (eq. 2) R_s	R_{nl} (eq. 13)		
		f (from eq. 14)		ϵ
		R_{so}	a and b	a_1 and b_1
1	Measured	Eq. 18	$a = 1.35$; $b = -0.34$	Eq. 17 --
2	Measured	Eq. 5	$a = 1.35$; $b = -0.34$	Eq. 15 a_1 variable; $b_1 = 0.139$
3	Measured	Eq. 19	$a = 1.35$; $b = -0.34$	Eq. 17 --
4	Measured	Eq. 21	Variable	Eq. 17 --
5	Measured	Eq. 26	Variable	Eq. 15 a_1 variable; $b_1 = 0.139$
6	Measured	Eq. 18	Variable	Eq. 15 $a_1 = 0.35$; $b_1 = -0.14$
7	Measured	--	--	Eq. 17 --
8	Measured	--	--	Eq. 15 a_1 variable; $b_1 = 0.139$
9	Measured	--	--	Eq. 15 $a_1 = 0.35$; $b_1 = -0.14$
10	Measured	Eq. 5	Variable	Eq. 17 --
11	Measured	Eq. 26	$a = 1.35$; $b = -0.34$	Eq. 17 --
12	Measured	Eq. 18	Variable	Eq. 15 a_1 variable; $b_1 = 0.139$
13	Measured	Eq. 5	Variable	Eq. 15 $a_1 = 0.35$; $b_1 = -0.14$
14	Measured	Eq. 21	$a = 1.35$; $b = -0.34$	Eq. 15 a_1 variable; $b_1 = 0.139$
15 (eq. 27) ^[b]	Measured	--	--	-- --
16 (eq. 28) ^[b]	Measured	--	--	-- --
17 (eq. 29) ^[b]	Eq. 30	--	--	-- --
18	Eq. 12	Eq. 19	$a = 1.35$; $b = -0.34$	Eq. 15 $a_1 = 0.35$; $b_1 = -0.14$
19	Eq. 12	Eq. 19	Variable	Eq. 15 a_1 variable; $b_1 = 0.139$

^[a] All methods, except methods 15, 16, and 17, use the same form of equation 1 and calculate R_n as the difference between R_{ns} and R_{nl} . The ASCE-EWRI R_n method uses equations 1 through 10 to calculate R_n and is not included in the table as one of the 19 R_n methods.

^[b] R_{ns} is not calculated for equations 15, 16, and 17.

where

- ET_{ref} = standardized grass- or alfalfa-reference ET (mm d⁻¹)
- Δ = slope of saturation vapor pressure versus air temperature curve (kPa °C⁻¹)
- R_n = net radiation at the surface (MJ m⁻² d⁻¹)
- G = heat flux density at the soil surface (assumed zero for daily time step)
- T = mean daily air temperature (°C)
- u_2 = mean daily or hourly wind speed at 2 m height (m s⁻¹)
- e_s = saturation vapor pressure (kPa)
- e_a = actual vapor pressure (kPa)
- $e_s - e_a$ = vapor pressure deficit (kPa)
- γ = psychrometric constant (kPa °C⁻¹)
- C_n and C_d = numerator and denominator constants, respectively, that change with reference surface and calculation time step
- 0.408 = coefficient (m² mm MJ⁻¹).

The values of C_n and C_d for grass- and alfalfa-reference surface for daily time steps are presented in table 2. All ET_{ref} calculations were done on a daily basis. Measured RH_{max} , RH_{min} , T_{max} , and T_{min} values were used to calculate e_a and e_s . A value of 1.013×10^{-3} MJ kg⁻¹ °C⁻¹, which represents an average value of specific heat (c_p) at constant temperature, was used in the calculations; γ was computed as a function of atmospheric pressure (P), c_p , and ratio of molecular weight of water vapor to dry air (0.622) for each study site, and P was calculated as a function of station elevation, z (m) as:

Table 2. Values of C_n and C_d for grass and alfalfa reference for daily and hourly time steps as reported by ASCE-EWRI (2005).^[a]

Time Step	Grass Reference (ET_o)		Alfalfa Reference (ET_r)	
	C_n	C_d	C_n	C_d
Daily	900	0.34	1600	0.38
Hourly during daytime	37	0.24	66	0.25
Hourly during nighttime	37	0.96	66	1.7

^[a] C_n is in units of °C mm s³ Mg⁻¹ d⁻¹ for 24 h time step and °C mm s³ Mg⁻¹ h⁻¹ for hourly time step. C_d is in units of s m⁻¹ for 24 h and hourly time step.

$$P = 101.3 \left(\frac{293 - 0.0065z}{293} \right)^{5.26} \quad (32)$$

RESULTS AND DISCUSSION

MEASURED RADIATION ENVELOPES

Measured radiation envelopes (R_s , R_n , and R_{nl}) for the 2005 and 2006 seasons for Clay Center are presented in figures 1a and 1b, respectively. R_s was the largest and R_{nl} was the smallest component of the radiation envelope. In general, R_s and R_n were largest in late July and decreased toward the end of the season. R_{nl} was smallest early in the season due to reduced reflection of radiation from the soil surface during partial canopy cover. R_{nl} increased toward the midseason as the canopy developed full closure, increasing reflection. R_{nl} ranged between 1.3 MJ m⁻² d⁻¹ in early June and about 5 MJ

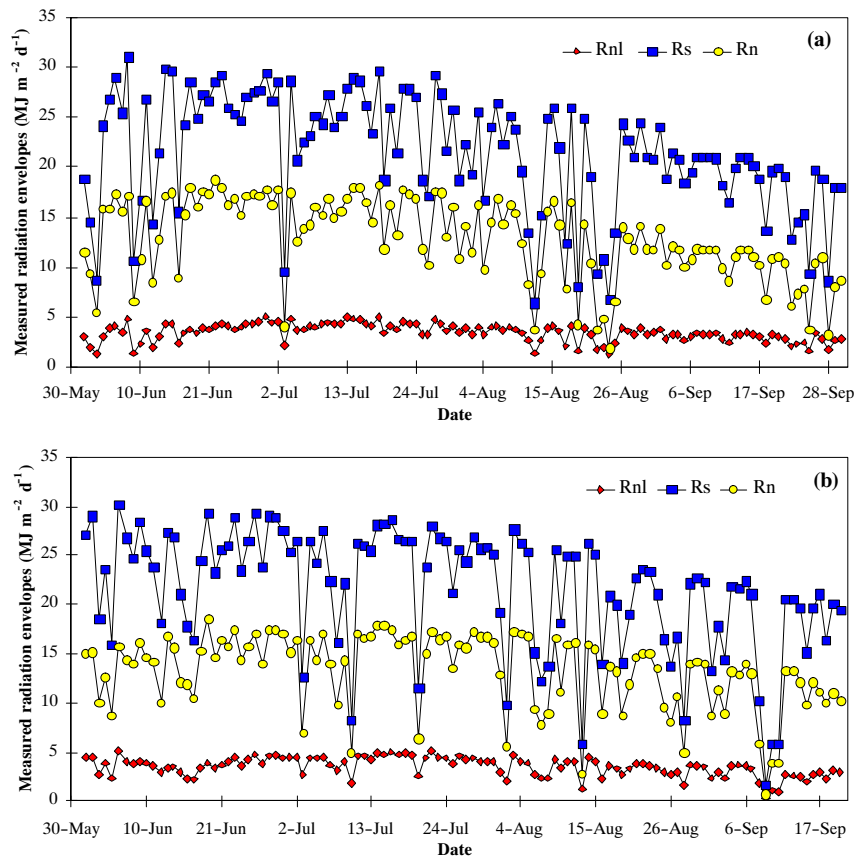


Figure 1. Seasonal distribution of measured daily radiation envelopes, including incoming shortwave radiation (R_s), net radiation (R_n), and outgoing net longwave radiation (R_{nl}) for the (a) 2005 and (b) 2006 seasons.

$\text{m}^{-2} \text{d}^{-1}$ in mid-to-late July in both years. The largest day-to-day variability was in R_s , as a function of cloud cover, and R_s ranged from 6.4 to 31.1 $\text{MJ m}^{-2} \text{d}^{-1}$ in 2005 and from 1.7 to 30.7 $\text{MJ m}^{-2} \text{d}^{-1}$ in 2006, with seasonal averages of 12.8 and 13.3 $\text{MJ m}^{-2} \text{d}^{-1}$ for 2005 and 2006, respectively. Overall, the maximum values of the radiation components were greater in 2005 due to less cloud cover, but the seasonal average values were greater in 2006. When the two years of data are pooled, on a seasonal average basis, R_n was about 60% of R_s . R_{nl} represented a small portion of R_s due to the interception of R_s at the surface and diffusion within the canopy. R_{nl} was about 16% of R_s in both years. R_n started to decrease from middle to late August in both seasons. During this time, leaf aging and senescence started reducing the α and R_n of the canopy due to increase in R_{ns} and due to a reduced amount of R_s toward the end of the season.

MEASURED ALBEDO AND TESTING THE HYPOTHESIS OF THE ALBEDO SIMILARITY BETWEEN MAIZE AND GRASS/ALFALFA CANOPIES

We present the seasonal distribution of daily α data measured over maize canopy in figure 2 for 2005 and 2006. Daily α values were obtained from hourly ratios of outgoing shortwave to incoming shortwave radiation. Hourly α values were obtained for a given day when $R_s > 0$ and averaged for the day. In 2005, the α increased gradually from approximately 0.15 early in the season to a maximum of around 0.23 in mid-season and gradually decreased to a range of 0.16 to 0.18 at the end of September during physiological maturity. The minimum α occurred on 4 June as 0.14, and the maximum occurred on 3 July, 26 July, and 12 August as 0.23. We observed similar trends in 2006. The seasonal average α was the same (0.19) in both years, which is 17% less than the commonly used value of 0.23 for grass and alfalfa surface. Our results are comparable with those reported by other researchers. Monteith (1959) made extensive measurements of surface α for various vegetation and reported α values for grass as 0.24 to 0.26, alfalfa as 0.16 to 0.22, and for 0.60 to 2.1 m tall maize canopy as 0.16 to 0.17. Monteith and Unsworth (1990) reported an average α of 0.24 for grass and 0.18 to 0.22 for maize canopy. Brutsaert (1982) grouped grass and other short green plants (maize, alfalfa, potatoes, beets) under the same category and reported an α range of 0.15 to 0.25 for these surfaces. Sellers (1965) and Oke (1978) grouped most of the green agronomical plants into one group

and suggested an α range of 0.10 to 0.25. Thus, it appears that α values reported in the literature for maize, grass, and alfalfa are very similar and vary in a narrow range.

Penman (1956) and Penman et al. (1967) suggested that the changes in plant color have very little influence on α and that the differences in ET caused by differences in α for agronomical vegetation are quite modest. Most agronomical vegetation surfaces have similar color. Grass and maize are both C4 grass-type plants and have similar plant physiological functions. Thus, one would expect the α values to be similar for both surfaces (Penman, 1956). It was an important step for us to demonstrate whether this assumption holds when comparing the measured R_n data over the maize canopy and estimated R_n data using grass-reference α (0.23) from all 20 R_n methods to quantify how much potential difference between the two R_n values are due to measurement of R_n over maize rather than grass canopy. We tested our hypothesis of α values being similar for maize and grass canopies and that slight differences would not cause significant differences in R_n , ET_o , and ET_r calculations in two ways. First, we estimated R_n using 2005 data for Clay Center from measured climatic variables for $\alpha = 0.23$ and $\alpha = 0.19$ (fig. 3). The α value of 0.19 is the seasonal average value that we measured over the maize canopy in both seasons. The two R_n estimations were within 6%, with R_n estimated using $\alpha = 0.19$ having the larger estimates. The two R_n estimations had a small RMSD (0.89 $\text{MJ m}^{-2} \text{d}^{-1}$) and high r^2 (1.0). The magnitude of R_n estimated using $\alpha = 0.19$ is greater than that of R_n estimated using $\alpha = 0.23$, using $\alpha = 0.23$, and the difference between the two R_n values increases at larger R_n values to a maximum difference of 6%. Based on the paired sample t-test (two-samples for means), the two R_n values were not significantly different at the 5% significance level ($p > 0.05$, table 3), supporting our hypothesis.

We quantified the impact of using $\alpha = 0.19$ instead of $\alpha = 0.23$ in calculation of R_n on ET_o and ET_r estimates using the ASCE-EWRI PM equation (eq. 31) for the 2005 data. Both daily ET_o and ET_r estimated using $\alpha = 0.23$ and $\alpha = 0.19$ exhibited the same seasonal trend with almost identical magnitude throughout the season (fig. 4). Regression analyses (fig. 5) showed that the ET_o values calculated using $\alpha = 0.23$ and $\alpha = 0.19$ were within 4% (fig. 5a) with a low RMSD of 0.22 mm d^{-1} , and the ET_r values were within 3% (fig. 5b) with a similar RMSD (0.21 mm d^{-1}). Thus, while using $\alpha = 0.19$ instead of $\alpha = 0.23$ resulted in 6% difference

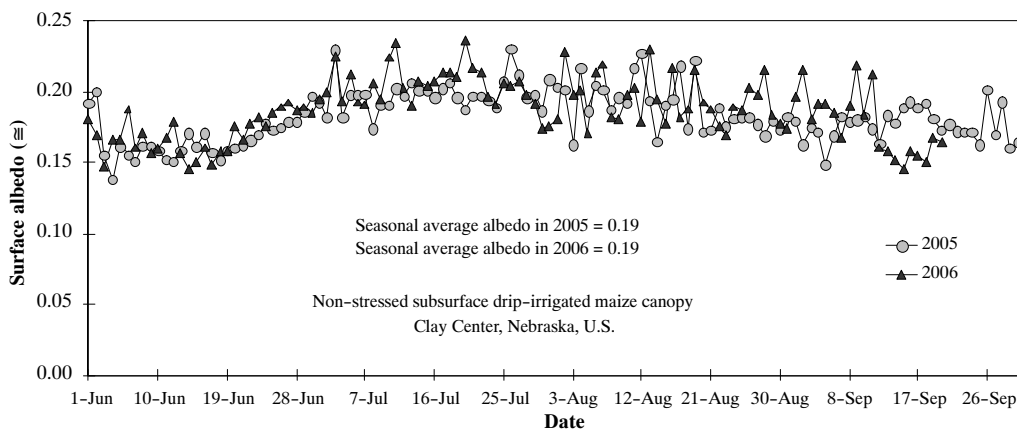


Figure 2. Seasonal distribution of daily surface albedo (α) over a non-stressed maize canopy for 2005 and 2006 growing seasons.

in R_n , this difference was translated to only 4% and 3% difference in ET_o and ET_r , respectively. The statistical analyses showed that the ET_o and ET_r values calculated using $\alpha = 0.23$ and $\alpha = 0.19$ were not significantly different ($p > 0.05$, paired sample t-test, table 3). The analyses of R_n , ET_o , and ET_r calculated using $\alpha = 0.23$ vs. $\alpha = 0.19$ indicated that our hypothesis that the α values for the maize and grass canopy are similar and that even some quantity of difference (17%) between the two would not cause a significant difference when computing R_n , ET_o , and ET_r is valid. Thus, we conclude that the performance of all 20 methods, which use $\alpha = 0.23$, can be statistically compared with the R_n data measured over maize canopy.

The statistical analyses results for autocorrelation for the residuals of regression between method-estimated R_n and the ASCE-EWRI-estimated R_n data and associated intercept and slopes are presented in table 4. Table 4 also includes the regress r-squared (RRS coeff.) between the residuals ASCE-EWRI R_n and method-estimated R_n , which ranges from 0 to 1. The outputs of the first-order Durbin-Watson test (DW) for significance are also included. The results are significant with positive autocorrelation ($p < 0.05$) for methods 4, 7, 8, 9, 10, 13, 15, and 18 at Clay Center, whereas seven methods (4, 7, 8, 9, 10, 15, and 16) had significant autocorrelation at Davis.

COMPARISONS OF ESTIMATED DAILY R_n FROM 19 METHODS WITH ASCE-EWRI-ESTIMATED R_n

Figures 6 and 7 present the regression analysis comparing the performance of the 19 R_n methods with the ASCE-EWRI R_n for Clay Center and Davis, respectively. The relationships

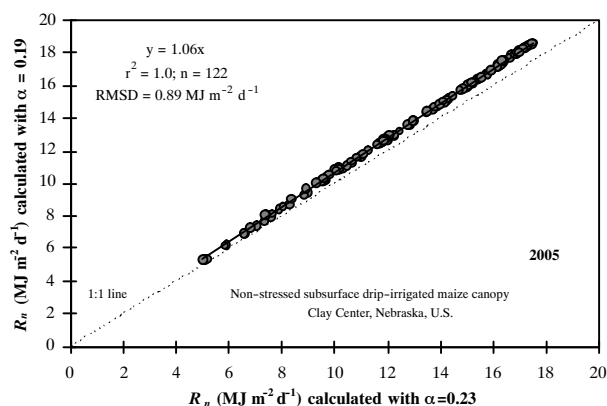


Figure 3. Relationship between net radiation (R_n) calculated using surface albedo (α) of 0.23 vs. R_n calculated using $\alpha = 0.19$ for a non-stressed maize canopy.

are presented in figures rather than in a tabular format to better visualize the data distribution in the entire range of R_n values and to better visualize the over- and underestimations in different R_n ranges. All methods, except for methods 15, 16, and 17, differ in estimating the cloudiness factor and ϵ for calculating R_{nl} . Overall, the majority of the methods had a good correlation with the ASCE-EWRI R_n ($r^2 > 0.95$). The RMSD values were less than $2 \text{ MJ m}^{-2} \text{ d}^{-1}$ for 12 methods at Clay Center and for 14 methods at Davis. The slope of the best-fit line ranged from 0.60 to 1.19 at Davis and from 0.76 to 1.37 at Clay Center. The RMSD ranged from 0.45 to $7.16 \text{ MJ m}^{-2} \text{ d}^{-1}$ at Davis and from 0.44 to $5.68 \text{ MJ m}^{-2} \text{ d}^{-1}$ at Clay Center. The performance of some of the methods showed

Table 3. Statistical analyses (two-tailed t-test for two-sample for means) between the R_n , ET_o , and ET_r values calculated using two surface albedo values ($\alpha = 0.23$ vs. $\alpha = 0.19$ for each pair variable). Analyses were done for 2005 season using the data from 1 June to 30 September ($n = 122$ for each case).

Variable	Mean		Variance		t-test (two-tail)		p-Value (p<0.05) ^[a]
	$\alpha = 0.23$	$\alpha = 0.19$	$\alpha = 0.23$	$\alpha = 0.19$	t_{computed}	t_{critical}	
Net radiation (R_n)	12.7	13.5	11.97	13.57	-1.884	0.0596	0.0596 ^{NS}
Grass-reference ET (ET_o)	4.86	5.07	2.23	2.38	-1.075	1.9599	0.2821 ^{NS}
Alfalfa-reference ET (ET_r)	6.10	6.30	4.39	4.55	-0.756	1.9599	0.4490 ^{NS}

[a] NS = not significant at 5% significance level.

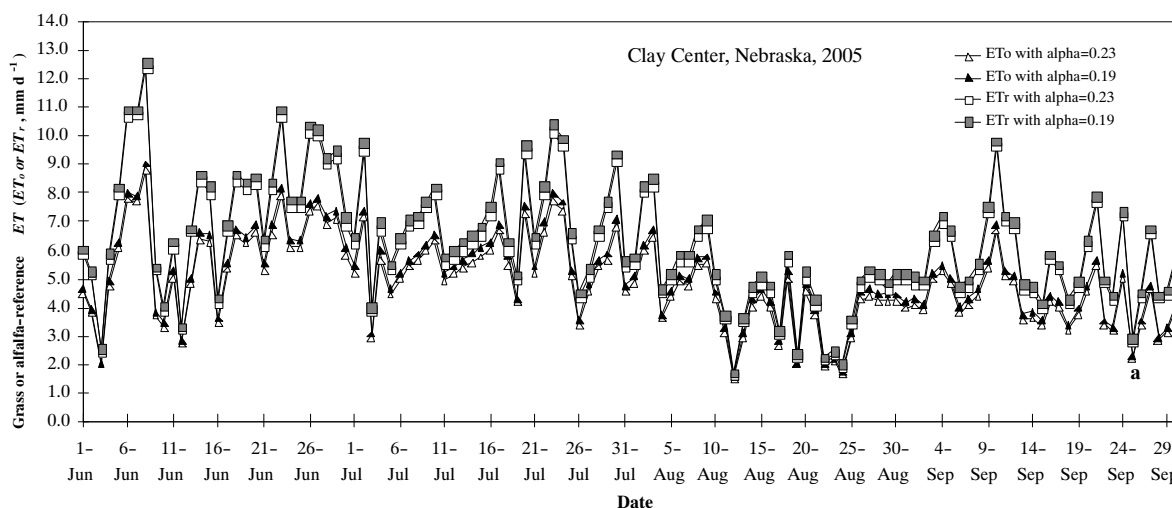


Figure 4. Grass- and alfalfa-reference evapotranspiration (ET_o and ET_r) calculated using surface albedo (α) of 0.23 versus 0.19 for 2005 growing season.

considerable variations between the two locations. For example, method 8 had a greater r^2 and lesser RMSD (0.78 and 3.72 MJ m⁻² d⁻¹, respectively) at Davis than at Clay Center ($r^2 = 0.57$ and RMSD = 5.28 MJ m⁻² d⁻¹), whereas method 17 performed better at Clay Center with r^2 of 0.78 and RMSD of 3.64 MJ m⁻² d⁻¹ than at Davis with r^2 of 0.85 but a much greater RMSD (7.16 MJ m⁻² d⁻¹). Methods 1, 6, 11, and 18 had the greatest r^2 values at Davis. Methods 1, 3, 11, and 18 had the greatest r^2 at Clay Center. In general, r^2 values were greater for Davis (semi-arid) than for Clay Center (sub-humid). The differences in the performance of the methods in two climates might be due to the differences in the influence of the climatic pattern on R_{nl} . Davis has less fluctuations in u_2 , T , RH , rainfall, and cloud cover during the summer months, whereas the fluctuations in these variables are very high in the summer months at Clay Center, contributing to differences in performance for some methods.

Methods 1, 3, 4, 6, 10, 11, 13, and 18 were very similar and were remarkably close to the ASCE-EWRI R_n calculations in both locations. For example, method 1 had an r^2 of 0.99 at both locations and RMSD of 0.44 MJ m⁻² d⁻¹ at Clay Center and 0.84 MJ m⁻² d⁻¹ at Davis. Method 1 overestimated ASCE-EWRI R_n only by 5% at Davis, whereas the slope of the regression line was 1.0 at Clay Center. Method 18 had an r^2 of 0.99 in both locations and underestimated ASCE-EWRI R_n by only 1%. It had RMSD of 0.47 and 0.45 MJ m⁻² d⁻¹ at Clay Center and Davis, respectively. The best performing equations (eqs. 6, 13, and 18) use equations 18, 5, and 19, respectively, to calculate R_{so} . They use equation 15 to calculate ϵ , and use constants a_1 and b_1 ($a_1 = 0.35$; $b_1 = -0.14$). Good performance of these methods in both locations that have different climatic patterns indicates the transferability of constants 0.35 and -0.14 between the locations and robustness of the procedures although they differed slightly in performance between the locations. This is most likely due to using the same constants in two different climatic conditions. Equations 1, 3, 4, 10, and 11 use different equations to calculate R_{so} , but they all use equation 17 to calculate ϵ as a function of mean air temperature, as developed by Idso et al. (1969) and Idso and Jackson (1969). By using equation 17 to calculate ϵ , all five equations had lower RMSD at Clay Center than Davis. The structure of methods 6, 13, and 18 are very similar to the ASCE-EWRI R_n procedures. They differ in estimating R_{so} and use different values for constants a , a_1 , b , and b_1 . The ASCE-EWRI uses $a = 1.35$, $b = -0.35$, $a_1 = 0.34$, and $b_1 = -0.14$. Since a single

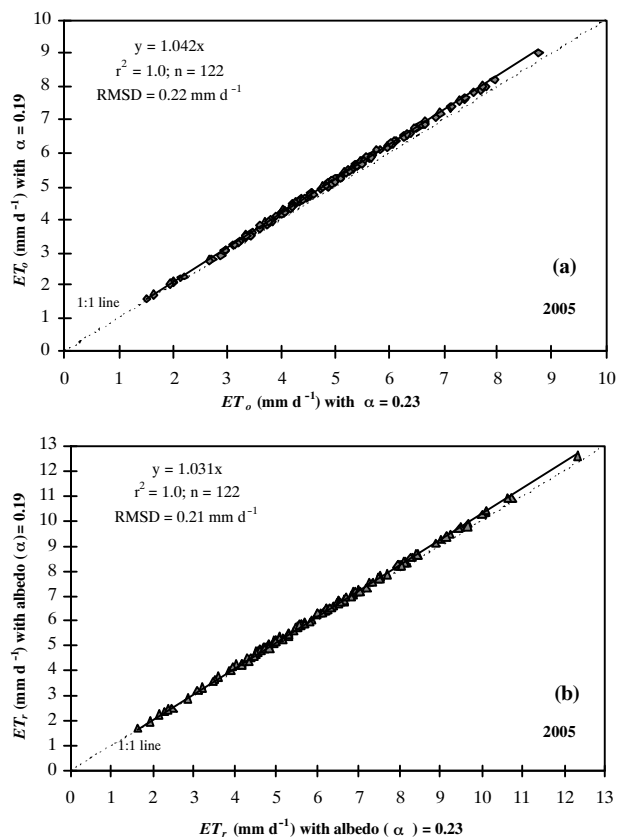


Figure 5. Relationship between (a) gross-reference evapotranspiration (ET_g) and (b) alfalfa-reference evapotranspiration (ET_r) as calculated using Penman-Monteith equation. Two sets of ET_g and ET_r values were calculated using net radiation (R_n) and surface albedo (α) of 0.23 and 0.19 to quantify the impact of two α values on ET_g and ET_r .

temperature measurement at the canopy height is used, the term $(0.34 - 0.14\sqrt{e_a})$ in equation 3 of the ASCE-EWRI R_n procedure should be similar to ϵ , representing the difference between the ϵ for the field and the effective ϵ for the surrounding atmosphere. The equation developed by Idso et al. (1969) and Idso and Jackson (1969) to estimate ϵ differs from the one used in the ASCE-EWRI R_n procedure in that it is more generalized, uses variable ϵ , and is based on a single canopy height mean air temperature, whereas the ASCE-EWRI procedure is based on the assumption that the ground

Table 4. Statistical analyses (autocorrelation, AC) between method-estimated net radiation (R_n) and ASCE-EWRI approach estimated R_n for Clay Center, Nebraska (1983-2004) and Davis, California (1990-2004). The autocorrelation analyses on residuals were conducted at the 5% significance level with null hypothesis that there is no first-order autocorrelation ($n = 8,036$ for Clay Center and $n = 5,479$ for Davis). The regress r-squared values (RRS coeff.) between the ASCE-EWRI R_n and method-estimated R_n are also included.

R_n Method	Clay Center, Nebraska					Davis, California				
	RRS Coeff.	DW Statistics	p-Value (p<0.05)	Intercept	Slope	RRS Coeff.	DW Statistics	p-Value (p<0.05)	Intercept	Slope
4	0.9846	1.8531	<0.05	0.7514	0.9417	0.9834	1.9399	<0.05	1.0655	0.8650
7	0.8706	1.5116	<0.05	3.9339	0.7445	0.9210	1.5289	<0.05	3.7566	0.6958
8	0.6919	1.6467	<0.05	4.9007	0.8572	0.9010	1.3710	<0.05	4.2775	0.7814
9	0.9123	1.5344	<0.05	3.9199	0.7616	0.9445	1.6155	<0.05	3.4632	0.7658
10	0.9846	1.8894	<0.05	0.7582	0.9758	0.9831	1.9479	<0.05	1.1418	0.8934
13	0.9969	1.9410	<0.05	0.9632	0.9652	--	--	--	--	--
15	0.8680	1.4501	<0.05	-0.0260	0.9673	0.9196	1.4799	<0.05	-0.3509	0.9279
16	--	--	--	--	--	0.9601	1.9419	<0.05	-0.7417	1.0043
18	0.9977	1.9300	<0.05	0.6958	0.9312	--	--	--	--	--

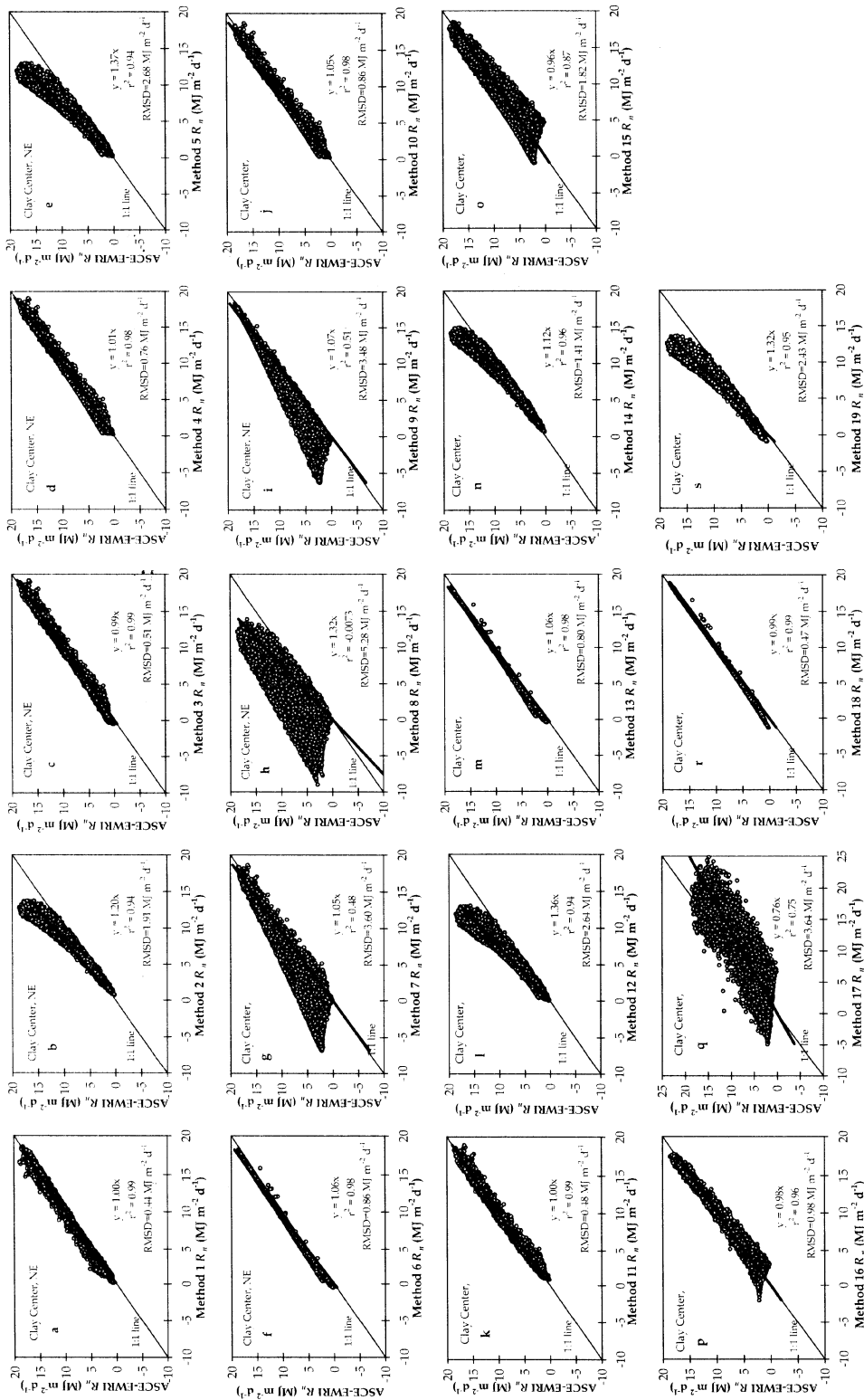


Figure 6. Relationship between the estimated daily R_n values using 19 methods and the ASCE-EWRI R_n values for calendar year for Clay Center, Nebraska ($n = 8,036$ for each case).

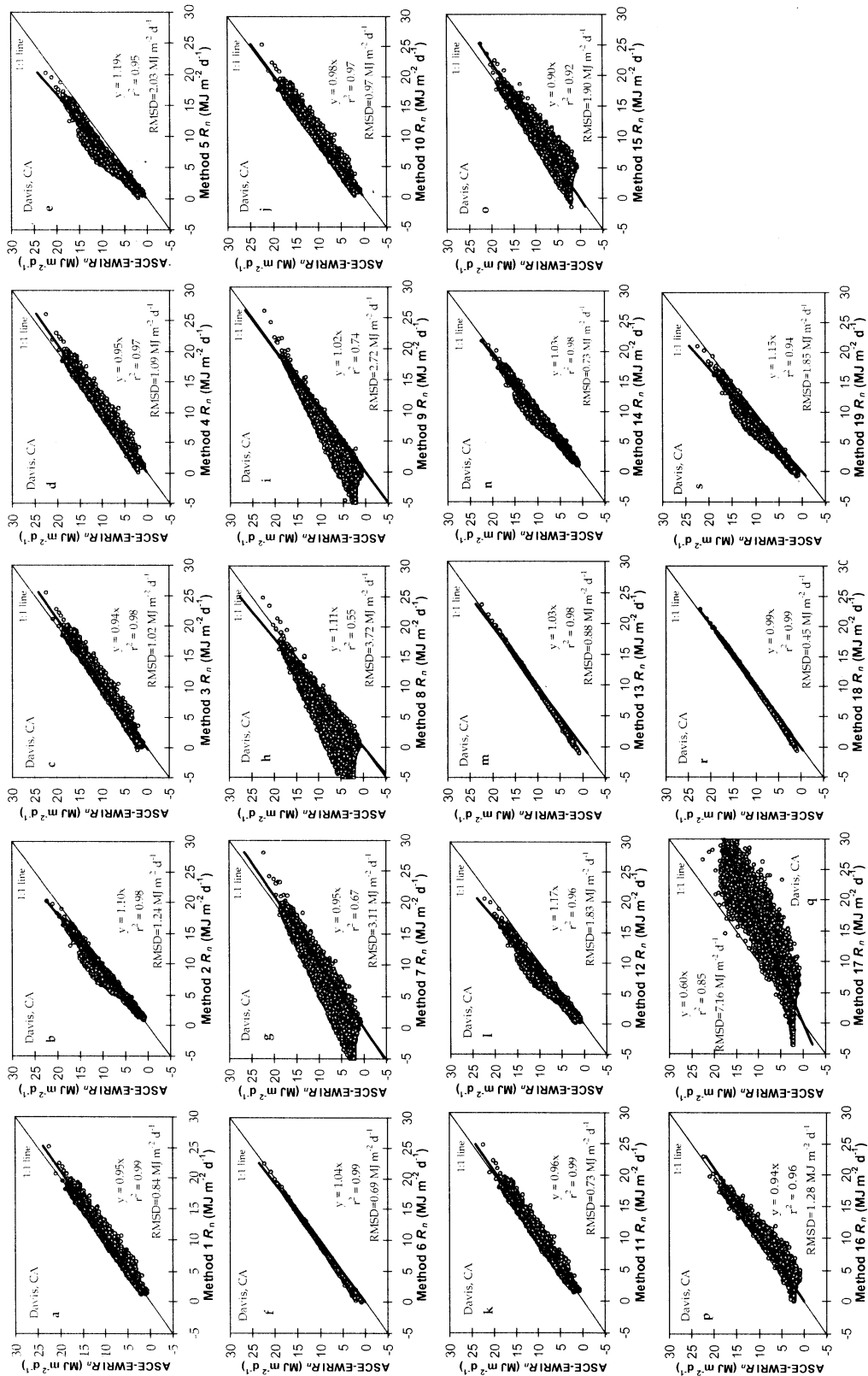


Figure 7. Relationship between the estimated daily R_n values using 19 methods and the ASCE-EWRI R_n values for the calendar year for Davis, California ($n = 5,479$ for each case).

and vegetation surface have a constant ϵ of 0.98. The ASCE-EWRI R_n procedure accounts for e_a , however.

The assumption $\epsilon = 0.98$ is valid for a mean air temperature of 21.1°C based on equation 17. However, the

mean air temperature can fluctuate plus or minus several degrees from 21.1°C during a growing season. As figure 8 shows, ϵ is a strong function of air temperature and ϵ can deviate from 0.98 substantially during the season as a

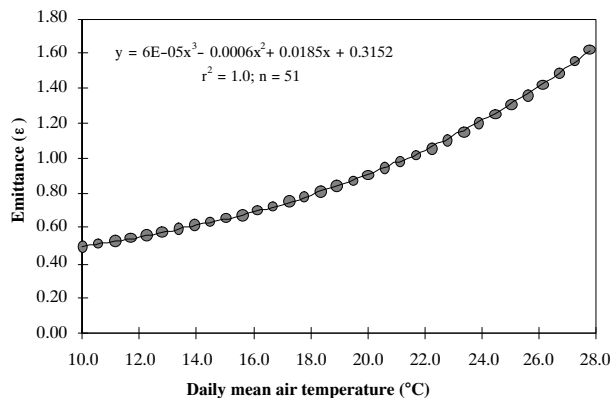


Figure 8. Relationship between emittance and mean air temperature.

function of changes in air temperature. While a constant $\epsilon = 0.98$ is the case for a green vegetation surface for the majority of the growing season, a variable ϵ as a function of air temperature should provide more realistic R_n values, because it will account for the impact of sudden temperature fluctuations on ϵ and R_n . Accounting for abrupt changes in air temperature is especially important in locations such as Clay Center, Nebraska, where fluctuations in weather variables are large. The slight differences in estimating R_{so} , ϵ , and other parameters resulted in slight differences in performance between equations 6, 13, and 18 and the ASCE-EWRI R_n at both study locations (figs. 6f, 1m, 1r, 2f, 2m, and 2r).

In figure 6, methods 7, 8, 9, and 15, and to a lesser extent method 16, exhibited a triangular-shaped distribution of the data (funnel effect) with larger scatter of data points in the lower range of R_n and narrower scatter with increasing R_n . This wide range of the R_n data scatter is usually observed in the non-growing (dormant) season. Irmak et al. (2003) observed similar trends and suggested that the larger deviations between the ASCE-EWRI R_n and the values computed from other methods were for smaller R_n than for larger R_n and might be due to using non-calibrated values of the parameters 0.75 and 2×10^{-5} (fractions of R_a reaching the earth on overcast days) in the calculation of R_{so} (eq. 5). Although turbidity and water vapor have some influence, especially for the smaller R_n values in the winter months, this influence is usually neglected in the empirical equations when computing R_{so} . As a result, it appears that none of the equations were able to fully account for the environmental factors described in R_{ns} and R_{nl} calculations, resulting in greater deviations from the ASCE-EWRI R_n data at a smaller R_n range. In addition, because most R_n methods, including the ASCE-EWRI, were developed for estimating R_n over green vegetation, the methods appear to fail in winter since most of them did not predict any negative R_n values in winter. Negative R_n values are usually recorded in winter on relatively clear, cold, and dry days with snow and/or ice cover on the ground due to greater surface albedo and with lower sun angles and changes in effective sky emittance, which would be the case at Clay Center. In summer, methods 7, 8, 9, and 15 underestimated R_n , suggesting that the effect of cloud cover attenuation of R_s is more significant in summer than in winter.

At Clay Center, methods that used equation 17 to estimate ϵ had the lowest RMSD values. Thus, equation 17, which

requires only mean air temperature to predict ϵ , provided more accurate R_n estimates as compared with equation 14, which uses actual vapor pressure. In figures 6 and 7, methods 2, 5, 12, 14, and 19 exhibited a distinct structure of data distribution of near-parabolic shape. These five methods use the same equation (eq. 12) for estimating ϵ , and the parameters a_1 and b_1 were computed as variable regression coefficients. The protruding data points were observed to be mainly the values for the period of March-April and early May over the 14-year period, suggesting that the performances of these methods were different in the spring. Method 16, developed by Irmak et al. (2003) for a different location (Florida), compared well with the ASCE-EWRI R_n method ($r^2 = 0.95$ and 0.96 at Davis and Clay Center, respectively, and RMSD of $1.28 \text{ MJ m}^{-2} \text{ d}^{-1}$ for Davis and $0.96 \text{ MJ m}^{-2} \text{ d}^{-1}$ for Clay Center), given that it uses the least number of input variables (T_{max} , T_{min} , and R_s) and had only 6% and 2% overestimation at Davis and Clay Center, respectively.

Methods 7, 8, and 9 compared poorly to ASCE-EWRI R_n calculations, with the lowest r^2 at both locations. Particularly, these methods had a cloudiness factor (f) of 1.0, which represents completely cloudy conditions. The effect of cloud cover errors can be subjective, although these conditions are known to attenuate R_s reaching the earth surface, which explains, in part, the underestimation of ASCE-EWRI R_n by these methods. At both locations, method 17 had the highest RMSD value and overestimated ASCE-EWRI R_n by 40% at Davis and by 24% at Clay Center. Method 17 was the only method that required estimated R_s , consequently deteriorating its performance as compared with the other methods, which use measured R_s . Its performance directly and strongly depends on the accuracy of R_s estimates. Daily values of R_s for method 17 were calculated using the procedures developed by Hargreaves and Samani (1982). The comparison of the Hargreaves and Samani method (HS)-estimated daily R_s values with the measured values from 1983 to 2004 for Clay Center and from 1990 to 2004 for Davis for the calendar year are presented in figures 9a and 9b, respectively. Performance of the HS R_s method was significantly different between the two locations. While the estimated R_s values for Clay Center were within 7% (underestimation) of the measured R_s values, the HS estimates had a large standard deviation ($7.53 \text{ MJ m}^{-2} \text{ d}^{-1}$), a low r^2 of 0.66, and a large RMSD of $4.31 \text{ MJ m}^{-2} \text{ d}^{-1}$ ($n = 8,036$) (fig. 9a). The magnitude of RMSD and standard deviation was greater at lower R_s values ($\leq 12 \text{ MJ m}^{-2} \text{ d}^{-1}$). Although the r^2 was 0.90 at Davis (fig. 9b), the method's estimate was poorer at Davis, with a larger RMSD and standard deviation. The method overestimated R_s by 19%. The magnitude of overestimations increased in the higher R_s range ($\geq 33 \text{ MJ m}^{-2} \text{ d}^{-1}$). The HS parameters were applied for both Clay Center and Davis without any correction or local calibration. The poor R_n estimates using method 17 suggest that the HS method parameters must be calibrated for a local region or climate, since only mean air temperature was not able to accurately account for variations in R_s at both locations.

COMPARISONS OF ESTIMATED DAILY R_n FROM 20 METHODS WITH MEASURED R_n AT CLAY CENTER

While the evaluation of the performance of different R_n methods relative to the ASCE-EWRI R_n method can provide

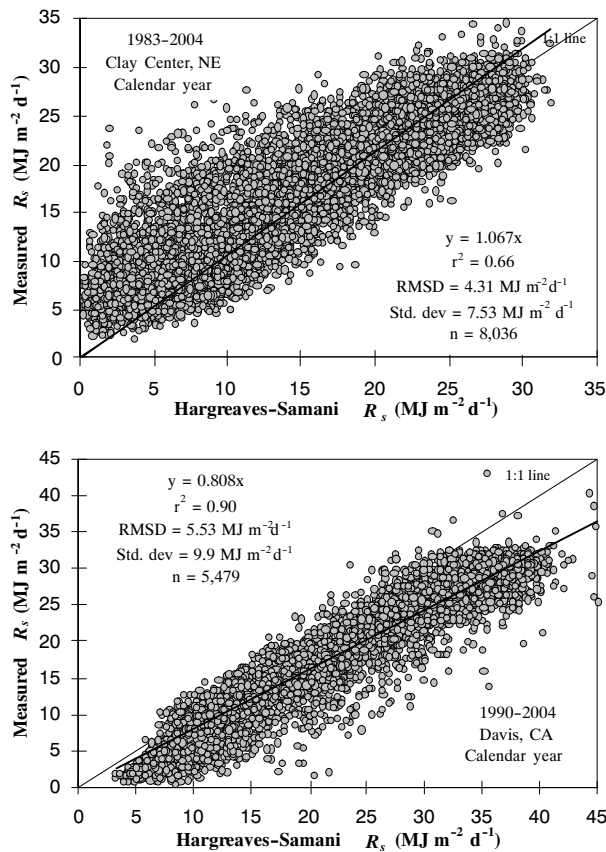


Figure 9. Estimated incoming shortwave solar radiation (R_s) using Hargreaves and Samani (1982) method for Clay Center, Nebraska (a) and Davis, California (b).

important information regarding the dynamics and effects of different parameters and coefficients involved in R_n estimates, their performance evaluations, including the ASCE-EWRI R_n values, against measured R_n is needed. Performance evaluation of different R_n methods can provide valuable information on alternative methods to the ASCE-EWRI R_n method, depending on the availability and quality of the climate data used in R_n estimations. However, the information on the operational performance and characteristics of the ASCE-EWRI R_n method itself against measured values has not been studied sufficiently. We compared the performance of all 20 R_n methods, including the ASCE-EWRI R_n values, with measured daily R_n values for a period of two growing seasons at Clay Center, and results are presented in figure 10. Figure 10 presents pooled data for the two growing seasons from 2005 and 2006. The results of statistical analyses are presented in table 5.

Overall, estimated R_n values correlated well with the measured data for most methods. Except for method 17, all methods underestimated measured R_n by a range of 6% to 23%. The R_n estimates from six methods (methods 1, 3, 11, 16, 18, and ASCE-EWRI) were not significantly different ($p > 0.05$) from those measured values at the 5% significance level (table 5). The r^2 values ranged from 0.64 (methods 7 and 17) to 0.95 (method 15), and the RMSD values ranged from 1.38 $\text{MJ m}^{-2} \text{d}^{-1}$ (method 18) to 4.83 $\text{MJ m}^{-2} \text{d}^{-1}$ (method 8). The ASCE-EWRI R_n values correlated well with the measured values ($r^2 = 0.93$), and the estimates were within 7% of the measured R_n . Methods 18, 3, ASCE-EWRI, 16, and 4 resulted in the lowest RMSD values (1.38, 1.40, 1.44, 1.46, and 1.49 $\text{MJ m}^{-2} \text{d}^{-1}$, respectively) and slopes closest to 1.0 ($r^2 \geq 0.86$) compared to the other methods. The estimates by method 16 (eq. 28) and ASCE-EWRI were very similar in both years. Method 16 was developed and calibrated by Irmak et al. (2003) using the FAO R_n procedures (Allen et al., 1998), which are the same as the ASCE-EWRI R_n procedures

Table 5. Statistical analyses (paired t-test for two-sample for means) between measured and model-estimated R_n for 2005 and 2006 seasons (pooled data) for Clay Center, Nebraska. Analyses were done for 2005 season using measured R_n data from 1 June to 30 September at 5% significance level. The hypothesized mean difference was zero ($n = 244$ for each case).

R_n Method	Mean		Variance		t-test t_{computed}	p-Value ($P_{0.05}$) ^[a]
	Estimated R_n	Measured R_n	Estimated R_n	Measured R_n		
1	11.9	12.8	12.9	16.7	-2.59	0.1150 ^{NS}
2	10.9	12.8	9.3	16.7	-5.65	0.0001*
3	12.2	12.8	13.8	16.7	-1.93	0.4390 ^{NS}
4	11.8	12.8	15.1	16.7	-3.00	0.0380*
5	9.9	12.8	10.5	16.7	-8.48	0.0001*
6	11.3	12.8	13.1	16.7	-4.48	0.0001*
7	9.8	12.8	24.8	16.7	-8.95	0.0001*
8	8.1	12.8	20.7	16.7	-13.91	0.0001*
9	9.9	12.8	21.4	16.7	-8.72	0.0001*
10	11.4	12.8	14.2	16.7	-4.17	0.0006*
11	11.9	12.8	13.3	16.7	-2.82	0.0641 ^{NS}
12	10.0	12.8	10.1	16.7	-8.23	0.0001*
13	11.4	12.8	13.2	16.7	-4.27	0.0004*
14	11.5	12.8	10.4	16.7	-3.94	0.0015*
15	11.4	12.8	14.0	16.7	-4.20	0.0005*
16	12.2	12.8	9.6	16.7	-1.73	0.5978 ^{NS}
17	15.2	12.8	14.5	16.7	6.95	0.0001*
18	12.1	12.8	13.2	16.7	-2.09	0.3365 ^{NS}
19	10.3	12.8	11.2	16.7	-7.43	0.0001*
ASCE-EWRI	12.0	12.8	12.3	16.7	-2.47	0.1534 ^{NS}

^[a] NS = not significant, and* = significant at the 5% significance level.

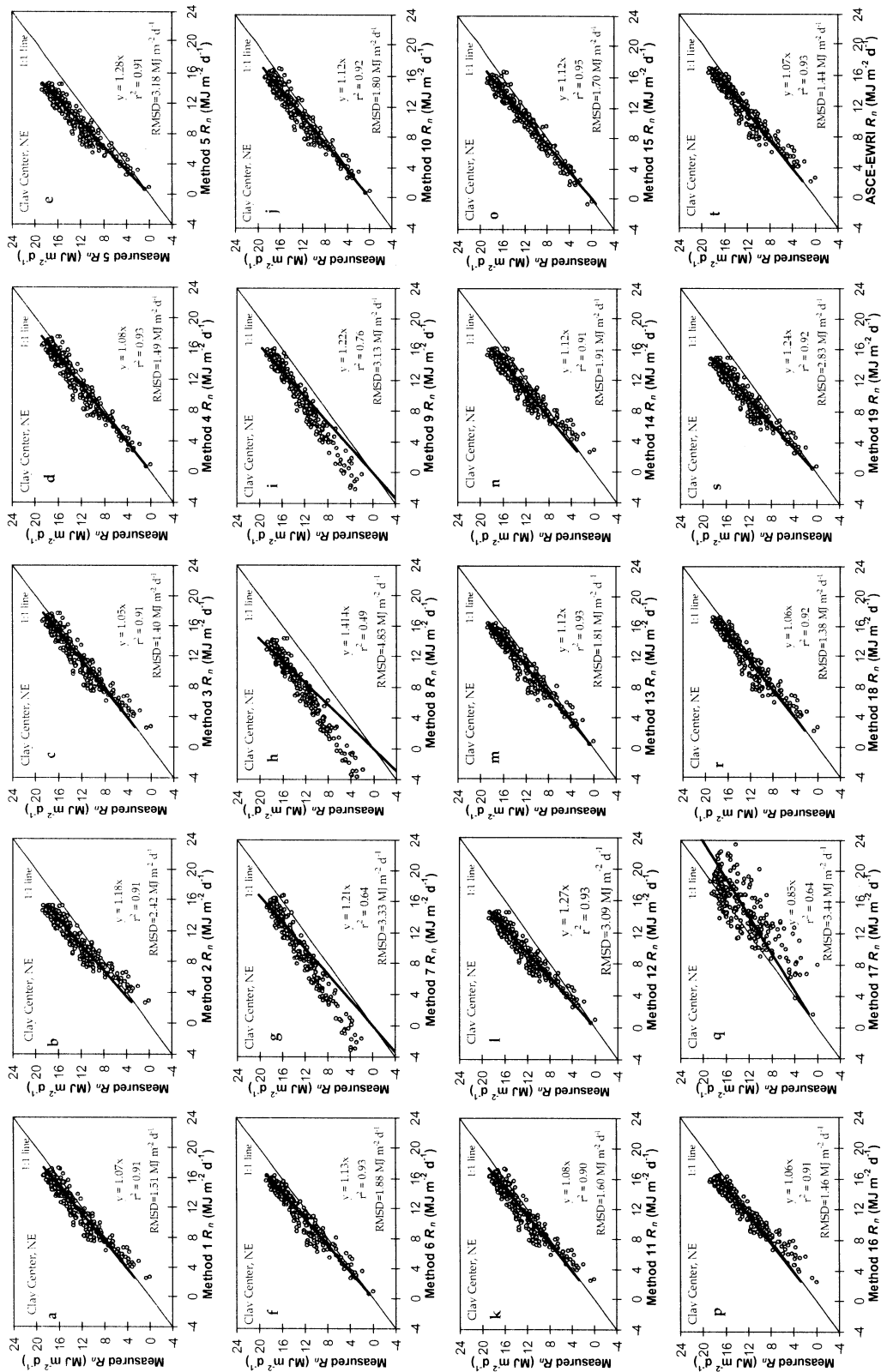


Figure 10. Regression analysis and the root mean square difference (RMSD) between the measured daily R_n and estimated R_n (19 methods and the ASCE-EWRI R_n procedure) for 2005 and 2006 growing seasons (1 June to 30 Sept., $n = 244$) (pooled data for two years) for Clay Center, Nebraska.

when applied on a daily time step for a reference humid location site. Method 16 (eq. 28) has an advantage over ASCE-EWRI in that it requires fewer inputs and can be a viable method for

estimating R_n when climate data are limited. The ASCE-EWRI method underestimated in the lower R_n range ($\leq 12 \text{ MJ m}^{-2} \text{ d}^{-1}$) and overestimated for values greater than $12 \text{ MJ m}^{-2} \text{ d}^{-1}$.

MEASURED VS. ESTIMATED NET LONGWAVE RADIATION (R_{nl}) AND SENSITIVITY OF R_n , ET_o , AND ET_r TO R_{nl}

A reason for the differences between estimated and measured R_n for most methods was attributed to the errors in estimation of R_{nl} . Further analyses were conducted to quantify the differences between method-estimated R_{nl} and ASCE-EWRI-estimated R_{nl} . Additional analyses were conducted to quantify the differences between the method-estimated R_{nl} , including the ASCE-EWRI R_{nl} , with the measured R_{nl} for Clay Center (table 6). With the exception of methods 5, 7, 8, 9, 12, and 19, the methods appeared to correlate reasonably with the ASCE-EWRI R_{nl} . However, the comparisons between the method-estimated R_{nl} , including the ASCE-EWRI R_{nl} , resulted in poor correlations with the measured values. The greatest r^2 was obtained from methods 6, 12, and 13 as 0.57. Models 6 and 13 had the least RMSD (1.19 and 1.23 MJ m⁻² d⁻¹, respectively). All methods had RMSD values greater than 1.0 MJ m⁻² d⁻¹, and two methods had RMSD greater than 2.0 MJ m⁻² d⁻¹. The ASCE-EWRI-estimated R_{nl} correlated poorly with the measured values ($r^2 = 0.47$, RMSD = 1.52 MJ m⁻² d⁻¹), and it overestimated by 27%. Consequently, these errors in estimated R_{nl} are reflected in R_n estimation when comparing any methods' performance against the ASCE-EWRI R_n , and when comparing all methods, including the ASCE-EWRI R_n , with the measured values. However, although poor correlations were observed between the measured and estimated R_{nl} , most methods' R_n estimates were judged to be good. This is because, compared to net shortwave radiation, R_{nl} is a small quantity of the net radiation balance, which might explain the marginal impact of the errors in R_{nl} estimation on R_n .

Table 6. Correlation between method-estimated R_{nl} and ASCE-EWRI R_{nl} estimates, and the method-estimated R_{nl} , including the ASCE-EWRI-estimated R_{nl} with the measured R_{nl} for maize canopy at Clay Center, Nebraska (regression equation where method-estimated $R_{nl} = \text{slope} \times \text{method-estimated or measured } R_{nl}$; $n = 244$). Data are for two growing seasons: from 1 June to 30 September 2005 and from 1 June to 20 September 2006.

R_{nl} Method	Method R_{nl} vs. ASCE-EWRI R_{nl} ^[a]			Method R_{nl} with ASCE-EWRI R_{nl} vs. measured R_{nl} ^[b]		
	Slope	r^2	RMSD ^[c]	Slope	r^2	RMSD ^[c]
1	0.99	0.93	0.40	1.25	0.35	1.68
2	0.77	0.92	1.19	0.97	0.42	1.28
3	1.06	0.92	0.48	1.31	0.24	1.89
4	0.99	0.87	0.57	1.25	0.44	1.61
5	0.66	0.87	2.00	0.84	0.53	1.50
6	0.87	0.96	0.65	1.10	0.57	1.19
7	0.62	0.05	2.63	0.83	0.12	2.02
8	0.49	0.08	3.99	0.65	0.11	3.06
9	0.65	0.28	2.34	0.86	0.26	1.65
10	0.90	0.87	0.72	1.14	0.50	1.34
11	0.98	0.92	0.44	1.22	0.27	1.69
12	0.67	0.87	1.95	0.86	0.57	1.39
13	0.88	0.96	0.58	1.12	0.57	1.23
14	0.87	0.93	0.66	1.10	0.35	1.42
18	1.04	0.99	0.20	1.29	0.31	1.79
19	0.71	0.88	2.57	0.90	0.52	1.30
ASCE-EWRI	--	--	--	1.27	0.47	1.52

[a] Comparison between method R_{nl} and ASCE-EWRI R_{nl} .

[b] Comparison between method R_{nl} (including ASCE-EWRI R_{nl}) and measured R_{nl} .

[c] RMSD is in units of MJ m⁻² d⁻¹.

To further analyze the effect of R_{nl} on R_n and on reference ET (ET_o and ET_r), we conducted a sensitivity analyses between these variables (fig. 11). We identified a typical summer day at Clay Center that had measured climatic variables of $T_{max} = 32^\circ\text{C}$, $T_{min} = 22^\circ\text{C}$, $RH_{max} = 93\%$, $RH_{min} = 40\%$, $R_s = 12 \text{ MJ m}^{-2} \text{ d}^{-1}$, and $u_2 = 4 \text{ m s}^{-1}$. From these variables, the ASCE-EWRI R_{nl} and R_n "base" values were calculated for the day as 0.13 and 1.41 MJ m⁻² d⁻¹, respectively. All other climatic variables were kept constant while changing R_{nl} . Based on these base climate data, the daily form of the PM equation (eq. 31) was used to calculate ET_o and ET_r values as 5.23 and 7.52 mm d⁻¹, respectively. The R_{nl} values were increased by 0.04 MJ m⁻² d⁻¹ increments up to 1.17 MJ m⁻² d⁻¹. For every 0.04 MJ m⁻² d⁻¹ increase in R_{nl} , we calculated the amount of change in R_n , ET_o , and ET_r (fig. 11). The R_{nl} effect on R_n was linear, and as expected, as R_{nl} increased, the R_n decreased. For every 0.04 MJ m⁻² d⁻¹ increase in R_{nl} , the R_n decreased by the same amount (0.04 MJ m⁻² d⁻¹). However, the effect of R_{nl} on ET_o and ET_r was subsidiary. An increase of 0.04 MJ m⁻² d⁻¹ in R_{nl} resulted in an increase of 0.06 mm in ET_o and ET_r . The change in R_{nl} affected ET_r slightly more than ET_o with a slightly greater slope, -1.39 for ET_r vs. -1.43 for ET_o , but the two slopes were not significantly different ($p > 0.05$). The range of increase in R_{nl} was from 0.04 to 1.17 MJ m⁻² d⁻¹, and this entire increase in R_{nl} resulted in a decrease in ET_r and ET_o of 1.49 and 1.45 mm, respectively. Similar to results of the R_n impact on ET_o and ET_r , the calculation of R_{nl} over a green maize canopy rather than over grass or alfalfa did not significantly influence ET_o or ET_r calculations.

SUMMARY AND CONCLUSIONS

We analyzed daily R_n values from 19 methods that differ in model structure and complexity. First, the estimates from all 18 methods were compared with the ASCE-EWRI R_n estimates in two climates: Clay Center, Nebraska (sub-humid) and Davis, California (semi-arid). As a second step, the R_n estimates from all 20 methods, including the ASCE-EWRI R_n values, were compared with the R_n values measured over an irrigated maize canopy at Clay Center. The majority of the models resulted in reasonable R_n estimates when compared to the ASCE-EWRI R_n values. The RMSD values between method-estimated and ASCE-EWRI-estimated R_n were lower than 2 MJ m⁻² d⁻¹ (0.82 mm d⁻¹) for 12 methods at Clay Center and for 14 methods at Davis. The performance of some of the methods showed considerable differences between the two locations. In general, the r^2 values were greater for the arid climate than for the sub-humid climate. Differences in model performance were attributed to differences in the influence of the general climatic patterns (more stable atmospheric conditions in summer in Davis than in Clay Center) on R_{nl} . When compared to the measured data, the ASCE-EWRI R_n values had one of the best agreements with the measured R_n data ($r^2 = 0.93$, RMSD = 1.44 MJ m⁻² d⁻¹), and its estimates were within 7% of the measured R_n . The R_n estimates from six methods, including ASCE-EWRI, were not significantly different ($p > 0.05$) from the measured R_n . Most methods underestimated measured R_n by a range of 6% to 23%. While the impact of R_{nl} on R_n is marginal, one reason for the differences between estimated and measured R_n for most

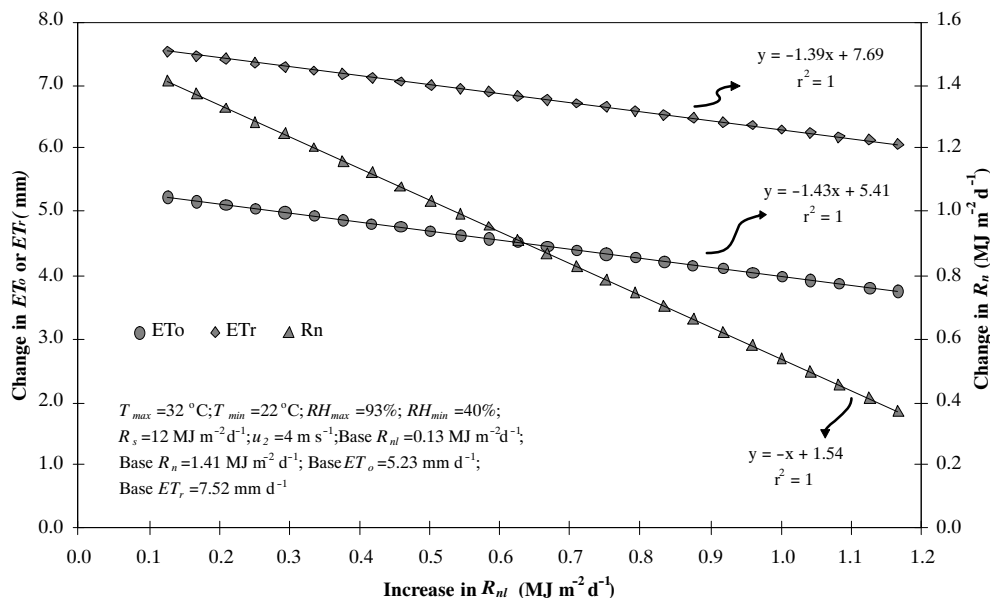


Figure 11. Relationship between net longwave radiation (R_{nl}), net radiation (R_n), grass-reference evapotranspiration (ET_o), and alfalfa-reference evapotranspiration (ET_r) for a clear summer day, Clay Center, NE.

methods was attributed to estimation of R_{nl} . The comparisons between the method-estimated R_{nl} with the measured values resulted in poor correlations. The ASCE-EWRI-estimated R_{nl} also correlated poorly with the measured values ($r^2 = 0.47$, $\text{RMSD} = 1.52 \text{ MJ m}^{-2} \text{ d}^{-1}$) with a 27% overestimation. The calculation of R_{nl} over a green maize canopy rather than over reference grass or alfalfa surfaces did not significantly influence ET_o or ET_r calculations. When the comparisons between the measured and model-estimated R_n values are considered, results suggest that the R_n data measured over green vegetation (e.g., irrigated maize canopy) can be an alternative R_n data source for ET estimations when measured R_n data are not available. Another alternative is using one of the R_n models that we analyzed when all the input variables are not available to solve the ASCE-EWRI R_n equation and when measured R_n data are not available. Our results can potentially be used to provide practical information on which method to select based on data availability for reliable estimates of daily R_n in climates similar to Clay Center and Davis.

REFERENCES

- Allen, R. G. 1997. Self-calibrating method for estimating solar radiation from air temperature. *J. Irrig. Drain. Eng.* 2(2): 56-67.
- Allen, R. G., L. S. Pereira, D. Raes, and M. Smith. 1998. Crop evapotranspiration: Guidelines for computing crop water requirements. FAO Irrigation and Drainage Paper No. 56. Rome, Italy: United Nations FAO.
- Angstrom, A. 1924. Solar and terrestrial radiation. *Q. J. Roy. Meteorol. Soc.* 50(210): 121-125.
- ASCE-EWRI. 2005. The ASCE standardized reference evapotranspiration equation. Standardization of Reference Evapotranspiration Task Committee Final Report. R. G. Allen, I. A. Walter, R. L. Elliot, T. A. Howell, D. Itenfisu, M. E. Jensen, and R. L. Snyder, eds. Reston, Va.: ASCE Environmental and Water Resources Institute (EWRI).
- Aubinet, M., B. Chermanne, M. Vandenhaute, B. Longdoz, M. Yernaux, and E. Laitat. 2001. Long-term carbon dioxide exchange above a mixed forest in the Belgian Ardennes. *Agric. Forest Meteorol.* 108(4): 293-315.
- Bowen, I. S. 1926. The ratio of heat losses by conduction and by evaporation from any water surface. *Phys. Rev.* 27(6): 779-787.
- Brunt, D. 1932. Notes on radiation in the atmosphere. *Q. J. Royal Meteorol. Soc.* 58(147): 389-418.
- Brutsaert, W. H. 1982. *Evaporation into Atmosphere*. Dordrecht, The Netherlands: D. Reidel Publishing.
- Deacon, E. L., and W. C. Swinbank. 1958. Comparison between momentum and vapor transfer. In *Climatology and Micrometeorology*, 38-41. UNESCO Arid Zone Research Series. Paris, France: UNESCO.
- Denmead, O. T., and I. C. McIlroy. 1970. Measurements of non-potential evaporation from wheat. *Agric. Meteorol.* 7: 285-302.
- Doorenbos, J., and W. O. Pruitt. 1977. Guidelines for prediction of crop water requirements. FAO Irrigation and Drainage Paper No. 24 (revised). Rome, Italy: United Nations FAO.
- Dyer, A. J. 1961. Measurements of evaporation and heat transfer in the lower atmosphere by an automatic eddy-correlation technique. *Q. J. Royal Meteorol. Soc.* 87(373): 401-412.
- Finnigan, J. J., R. Clemens, Y. Malhi, R. Leuning, and H. A. Cleugh. 2003. A re-evaluation of long-term flux measurement techniques: Part I. Averaging and coordinate rotation. *Boundary-Layer Meteorol.* 107(1): 1-48.
- Fuchs, M., and C. B. Tanner. 1970. Error analysis of Bowen ratio measured by psychrometry. *Agric. Meteorol.* 7: 329-334.
- Hargreaves, G. H., and Z. A. Samani. 1982. Estimating potential evapotranspiration. *J. Irrig. Drain. Eng. ASCE* 108(3): 223-230.
- Heermann, D. F., G. J. Harrington, and K. M. Stahl. 1985. Empirical estimation of clear sky solar radiation. *J. Climate and Applied Meteorol.* 24(3): 206-214.
- Hubbard, K. G. 1992. Climatic factors that limit daily evapotranspiration in sorghum. *Climate Research* 2(1): 73-80.
- Idso, S. B., and R. D. Jackson. 1969. Thermal radiation from the atmosphere. *J. Geophys. Res.* 74(23): 5397-5403.
- Idso, S. B., R. D. Jackson, W. L. Ehler, and S. T. Mitchell. 1969. A method for determination of infrared emittance of leaves. *Ecology* 50(5): 899-902.
- Irmak, S. 2010. Nebraska Water and Energy Flux Measurement, Modeling, and Research Network (NEBFLUX). *Trans. ASABE* 53(4): 1097-1115.

- Irmak, S., and D. Mutiibwa. 2008. Dynamics of photosynthetic photon flux density and light extinction coefficient for assessing radiant energy interactions for maize canopy. *Trans. ASABE* 51(5): 1663-1673.
- Irmak, S., A. Irmak, R. G. Allen, and J. W. Jones. 2003. Solar and net radiation-based equations to estimate reference evapotranspiration in humid climates. *J. Irrig. Drain. Eng. ASCE* 129(5): 336-347.
- Irmak, S., J. O. Payero, D. L. Martin, A. Irmak, and T. A. Howell. 2006. Sensitivity analyses and sensitivity coefficients of the standardized ASCE-Penman-Monteith equation to climate variables. *J. Irrig. Drain. Eng. ASCE* 132(6): 564-578.
- Irmak, S., D. Mutiibwa, A. Irmak, T. J. Arkebauer, A. Weiss, D. L. Martin, and D. E. Eisenhauer. 2008. On the scaling up leaf stomatal resistance to canopy resistance using photosynthetic photon flux density. *Agric. Forest Meteorol.* 148(6-7): 1034-1044.
- Jensen, M. E., R. D. Burman, and R. G. Allen. 1990. *Evapotranspiration and Irrigation Water Requirements*. ASCE Manuals and Reports on Engineering Practices No. 70. Reston, Va.: ASCE.
- Monteith, J. L. 1959. The reflection of short-wave radiation by vegetation. *Q. J. Royal Meteorol. Soc.* 85(366): 386-392.
- Monteith, J. L., and M. Unsworth. 1990. *Principles of Environmental Physics*. 2nd ed. London, U.K.: Edward Arnold.
- Murray, F. W. 1967. On the computation of saturation vapor pressure. *J. Appl. Meteorol.* 6(1): 203-204.
- Oke, T. P. 1978. *Boundary Layer Climates*. New York, N.Y.: John Wiley and Sons.
- Paw, U. K. T., J. Qui, H. B. Su, T. Watanabe, and Y. Brunet. 1995. Surface energy renewal analysis: A new method to obtain scalar fluxes without velocity data. *Agric. Forest Meteorol.* 74(1-2): 119-137.
- Penman, H. L. 1956. Evaporation: An introductory survey. *Netherlands J. Agric. Sci.* 4: 9-29.
- Penman, H. L., D. E. Angus, and C. H. M. Van Bavel. 1967. Microclimatic factors affecting evaporation and transpiration. In *Irrigation of Agricultural Lands*, 483-574. R. M. Hagan, H. R. Haise, and T. W. Edminster, eds. Agronomy Monograph No. 11. Madison, Wisc.: ASA.
- Samani, Z. 2000. Estimating solar radiation and evapotranspiration using minimum climatological data. *J. Irrig. Drain. Eng.* 126(4): 265-267.
- Sellers, W. D. 1965. *Physical Climatology*. Chicago, Ill.: University of Chicago, Press.
- Snyder, R. L., and W. O. Pruitt. 1992. Evapotranspiration data management in California. *Proc. ASCE Water Forum '92*, 128-133. Reston, Va.: ASCE.
- Snyder, R. L., D. Spano, and U. K. T. Paw. 1996. Surface renewal analysis for sensible and latent heat flux density. *Boundary-Layer Meteorol.* 77(3-4): 249-266.
- Snyder, R. L., D. Spano, P. Duce, U. K. T. Paw, and M. Rivera. 2008. Surface renewal estimation of pasture evapotranspiration. *J. Irrig. Drain. Eng.* 134(6): 716-721.
- Swinbank, W. C. 1951. Measurement of vertical transfer of heat and water vapor by eddies in the lower atmosphere. *J. Meteorol.* 8(3): 135-145.
- Tanner, C. B. 1960. Energy balance approach to evapotranspiration from crops. *SSSA Proc.* 24(1): 1-9.
- Thornton, P. E., and S. W. Running. 1999. An improved algorithm for estimating incident daily solar radiation from measurements of temperature, humidity, and precipitation. *Agric. Forest Meteorol.* 93(4): 211-228.
- Webb, E. K., G. I. Pearman, and R. Leuning. 1980. Correction of flux measurements for density effects due to heat and water vapour transfer. *Q. J. Royal Meteorol. Soc.* 106(447): 85-100.
- Wright, J. L. 1982. New evapotranspiration crop coefficients. *J. Irrig. Drain. Div. ASCE* 108(IR2): 57-74.
- Wright, J. L., and M. E. Jensen. 1972. Peak water requirements of crops in southern Idaho. *J. Irrig. Drain. Div. ASCE* 96(IR1): 193-201.

NOMENCLATURE

α	= albedo or canopy reflection coefficient
ϵ	= atmospheric emissivity
σ	= Stefan-Boltzmann constant (4.903×10^{-9} MJ K ⁻⁴ m ⁻² d ⁻¹)
ω_s	= sunset hour angle (rad)
φ	= latitude (rad)
δ	= solar declination angle (rad)
ϕ	= sun angle above the horizon (rad)
a	= 1.35
a_1	= 0.35
a_3	= 0.61
a_s	= 0.25
b	= -0.34
b_1	= -0.14
b_3	= -1.0
b_s	= -0.50
d_r	= inverse relative distance from earth to sun
e_a	= actual vapor pressure of the air (kPa)
f	= factor to adjust for cloud cover
G_{sc}	= solar constant (0.0820 MJ m ⁻² min ⁻¹)
K_B	= clearness index for direct beam radiation
K_D	= clearness index for diffuse beam radiation
K_t	= turbidity coefficient ($0 < K_t \leq 1.0$)
L	= latitude
m	= month of the year
N	= day of the year
n/N	= ratio of actual measured bright sunshine hours and maximum possible sunshine hours
P	= atmospheric pressure (kPa)
P_o	= mean monthly atmospheric pressure at sea level (kPa)
PM	= Penman-Monteith
R_a	= extraterrestrial radiation (MJ m ⁻² d ⁻¹)
R_s	= total incoming shortwave solar radiation (MJ m ⁻² d ⁻¹)
R_n	= net radiation (MJ m ⁻² d ⁻¹)
R_{so}	= calculated clear-sky solar radiation (MJ m ⁻² d ⁻¹)
R_{ns}	= incoming net shortwave radiation (MJ m ⁻² d ⁻¹)
R_{nl}	= outgoing net longwave radiation (MJ m ⁻² d ⁻¹)
RH_i	= average relative humidity (%)
T_i	= average air temperature (°C)
T_{max}	= maximum air temperature
T_{min}	= minimum air temperature
W	= precipitable water vapor in the atmosphere (mm)
z	= elevation (m)